



University  
of Stavanger

**MATHIAS SANDVIK**

**SUPERVISOR: ILKE PALA OZKOK**

# **Acute and Chronic impact of Bisphenols on Activated Sludge systems using Respirometry**

**Master thesis, 2024**

**Environmental Engineering**

**Faculty of Science and Technology**

**Department of Chemistry, Bioscience and Environmental Engineering**



## **Abstract**

Bisphenol A (BPA) is a compound produced mainly for polycarbonate plastic (PC). Due to its endocrine disruptive effects to humans and animals, industries have shifted to alternative BP analogues, namely Bisphenol F (BPF) and Bisphenol S (BPS). In order to find the effects that this has on wastewater treatment plants (WWTPs), seed sludge gathered from IVAR at SNJ Mekjarvik (Stavanger) were used to set up reactors to estimate the acute and chronic impact that BPA, BPF and BPS have on biological wastewater treatment systems by the use of respirometry and activated sludge modeling. Respirometry were used to measure the oxygen utilization rate (OUR) of the biomass and were exposed at the first time and after the chronic period an already established EC50 concentration of 30 mg BP/L and during the chronic period of 30 days with an environmental relevant concentration of 12 mg BP/L. Solids concentration, pH and COD removal was measured during operation time of all reactors. During respirometry tests, addition of BP analogues caused a significant decrease in OUR and worsened after the chronic period. It was found that the BP analogues caused competitive and un-competitive inhibition for growth, un-competitive inhibition for hydrolysis and non-competitive inhibition for storage on polyhydroxyalkanoates (PHA's). Furthermore, from chronic exposure, the endogenous decay rate increased while the activity of the biomass decreased from BP exposure. Finally, the solids concentration and COD removal decreased from BP addition. BPF and BPS had an equal or worse effect of that of BPA after chronic exposure.

## **Acknowledgements**

I would like to extend my deepest gratitude and appreciation to my supervisor Ilke Pala Ozkok for her endless support and superb guidance throughout my master thesis. You made the master thesis not only deeply educational, but also a pleasant time.

I would also thank Sumaiah Hussain for her excellent cooperation during my practical work. Your attention for detail, lab expertise and relaxed manner always made the lab experience a great time.

A deep appreciation also goes to Daniel Basiry and Erling Berge Monsen for their constant availability and great companionship during my master thesis.

Thanks to Sudikshya Shrestha, Viktorija Moreno and Halvor Sundal for great work ethic and eagerness to help, keeping me motivated during my lab work.

## ABBREVIATIONS

BP	Bisphenol
BPA	Bisphenol A
BADGE	Bisphenol A diglycidyl ether
BPS	Bisphenol S
BPF	Bisphenol F
WWTP	Wastewater Treatment Plant
Dw	dry weight
ASM3	Activated Sludge Model NO.3
TSS	Total Suspended Solids
VSS	Volatile Suspended Solids
SRT	Solid Retention Time
HRT	Hydraulic Retention Time
COD	Chemical Oxygen Demand
OUR	Oxygen utilization rate
Sol A	Phosphate buffer
PHA	Storage product called Polyhydroxyalkanoates
$\hat{\mu}_H$	Maximum growth rate for biomass
$K_S$	Half saturation constant for growth of biomass
$K_H$	Maximum hydrolysis rate for hydrolysable substrate
$K_X$	Hydrolysis half saturation constant for hydrolysable substrate
$k_{STO}$	Maximum storage rate of PHA by biomass
$\hat{\mu}_{STO}$	Maximum growth rate for biomass by PHA
$b_H$	Endogenous decay rate for biomass

## Table of Contents

ABBREVIATIONS .....	3
List of Figures .....	6
List of Tables .....	7
1. Introduction .....	8
2. Background .....	8
2.1 Bisphenol A .....	8
2.2 BP analogues .....	10
2.2.1 Bisphenol S .....	10
2.2.2 Bisphenol F .....	11
2.2.3 Endocrinal Disruptive effects of BP analogues.....	12
2.2.4 Biotransformation and biodegradation of BP analogues.....	13
2.3 Wastewater Treatment Plants and Activated Sludge System .....	17
2.4 Activated Sludge Modeling.....	18
2.4.1 Activated Sludge Modeling No.1 .....	19
2.4.2 Activated Sludge Modeling No.3 .....	20
2.4.3 Respirometry and Oxygen Utilization Rate (OUR) .....	23
2.5 Enzyme inhibition .....	23
2.5.1 Competitive inhibition.....	23
2.5.2 Non-competitive inhibition .....	23
2.5.3 Un-competitive inhibition .....	24
3. Materials and Methods .....	25
3.1 Reactor Setup and Operations .....	25
3.2 Experimental Procedures.....	27
3.2.1 Suspended Solids (SS) and Volatile Suspended Solids (VSS) .....	27

3.2.2 Chemical Oxygen Demand (COD) and Nitrate Nitrogen (NO <sub>3</sub> <sup>-</sup> -N) .....	27
3.2.3 pH measurement.....	27
3.2.4 Preparation of BP analogue stock solutions .....	28
3.2.5 Respirometry and Oxygen Utilization Rate (OUR) .....	28
4. Results & Discussions.....	30
4.1 Analysis of Test Results.....	30
4.1.1 Control Tests.....	30
4.1.2 Acute Tests .....	33
4.2 Chronic BP addition .....	36
4.2.1 Reactor Analysis.....	37
4.2.2 Degradation of BP analogues .....	39
4.2.3 Chronic BP .....	40
4.3 Activated Sludge Modelling Results .....	42
4.3.1 Control.....	42
4.3.2 Acute BP.....	45
4.3 Chronic BP .....	50
5. Conclusions and Future Recommendations .....	57
6. References .....	58
7. Appendix .....	62

## List of Figures

Figure 1 - General scheme of BP analogues. ....	9
Figure 2 - Reaction scheme of BPA. ....	9
Figure 3 - Scheme of BADGE .....	9
Figure 4 - Reaction scheme of BPS. ....	10
Figure 5 - Reaction scheme of BPF.....	10
Figure 6 – The major pathways of biotransformation of BPA .....	13
Figure 7 - Proposed bacterial metabolic pathway of BPA .....	15
Figure 8 – Proposed bacterial metabolic pathway for BPF.....	16
Figure 9 - Proposed bacterial metabolic pathway for BPS .....	17
Figure 10 - Diagram of storage process in ASM3.....	21
Figure 11 – Photograph of the control reactor.....	25
Figure 12 – Photograph of the chronic BPA (Left), BPF (Middle) and BPS (Right) reactors. ....	26
Figure 13 – Solids and pH analysis of the control reactor during operation.....	31
Figure 14 – COD removal efficiency of the control reactor during operation.....	32
Figure 15 – OUR and COD Profile from Experimental data of Control Reactor .....	33
Figure 16 – OUR and COD Profile from Experimental data with BPA addition.....	34
Figure 17 – OUR and COD Profile from Experimental data with BPF addition.....	35
Figure 18 – OUR and COD Profile from Experimental data with BPS addition.....	36
Figure 19 – Solids analysis during chronic BP addition .....	37
Figure 20 – COD removal during chronic BP addition.....	38
Figure 21 - OUR and COD Profile from Experimental data with chronic BPA addition .....	40
Figure 22 - OUR and COD Profile from Experimental data with BPF addition .....	41
Figure 23 - OUR and COD Profile from Experimental data with BPS addition .....	42
Figure 24 – Modelled OUR (Top) and COD (Bottom) Profiles of control using Aquasim .....	44

Figure 25 – Model simulation for OUR (Top) and COD (Bottom) Profiles of Acute BPA test .....	46
Figure 26 - Model simulation for OUR (Top) and COD (Bottom) Profiles of Acute BPF test	47
Figure 27 - Model simulation for OUR (Top) and COD (Bottom) Profiles of Acute BPS test	48
Figure 28 - Model simulation for OUR (Top) and COD (Bottom) Profiles of Chr. BPA test	51
Figure 29 - Model simulation for OUR (Top) and COD (Bottom) Profiles of Chr. BPF test..	53
Figure 30 - Model simulation for OUR (Top) and COD (Bottom) Profiles of Chr. BPS test..	55
Figure 31 – Temp. (Top), DO (Middle) and OUR (Bottom) Profiles from Chr. BPA test.....	63
Figure 32 – Temp. (Top), DO (Middle) and OUR (Bottom) Profiles from Chr. BPF test.....	65
Figure 33 – Temp. (Top), DO (Middle) and OUR (Bottom) Profiles from Chr. BPS test.....	67

### **List of Tables**

Table 1 - Matrix representation of ASM3 .....	22
Table 2- Composition of peptone mixture and Solution A.....	27
Table 3 – Concentrations of BP analogue stock solutions .....	28
Table 4 – Sampling intervals during an OUR test.....	29
Table 5 – Steady state values for solids concentration and COD removal in chronic BP reactors .....	39
Table 6 – COD data determined from R-test with only BP addition.....	39
Table 7 – Values of control models determined by model calibration .....	43
Table 8 - Values of acute models determined by model calibration.....	49
Table 9 - Values of chronic models determined by model calibration .....	56



## 1. Introduction

In the 1930s during the plastic revolution, the creation of the most popular plastic types that we know today were made. This includes polyvinylchloride and polyethylene. Although beneficial for society, the compromise of plastics that were transparent and soft and those that were hard and brittle became a motivation for further research. That was until the 1950s were polycarbonate (PC) was discovered. PC is a hard, tough, and transparent plastic that can tolerate high temperatures.<sup>1</sup> The main ingredient used in making PC plastic is the main scope of this thesis; Bisphenol A (BPA). Since EU has harshly reduced the production and use of BPA, there are alternatives that are in use instead of BPA during production of PC plastics. BPS and BPF are the most popular substitutes, of which the impact on wastewater treatment systems is unknown. The scope of this thesis is to determine the acute and chronic impact of BPA, BPS and BPF on biological wastewater treatment systems by the use of respirometry and activated sludge modeling.

## 2. Background

### 2.1 Bisphenol A

Bisphenols (BPs) are synthesized phenolic organic compounds. They consist of tails of phenols separated by an aliphatic or inorganic bridge (*Figure 1*). BPA was the first synthesized BP analogue by an acid catalyzed condensation reaction of phenol and acetone (*Figure 2*). As the main monomer in making PC plastic, BPA used to exist in everyday items such as water bottles, baby bottles and thermal paper used for receipts. Furthermore, BPA is also used as a reactant to make epoxy resins. The most popular resin used today is Bisphenol A diglycidyl ether (BADGE). BADGE is commonly used as an inner coating material in food and drink products.<sup>2</sup> It is synthesized by O-Alkylation of BPA with epichlorohydrin (*Figure 3*). From the period of 1996-1999, the estimated total polycarbonate and epoxy resin production from BPA in the EU was 560,000 tons/year, totaling 96% of all BPA production.<sup>3</sup> The annual production of BPA was estimated to be 5.5 million tons in 2011, signifying a dramatic increase in demand.<sup>4</sup>

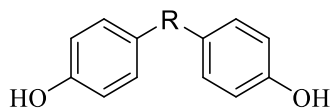


Figure 1 - General scheme of BP analogues.

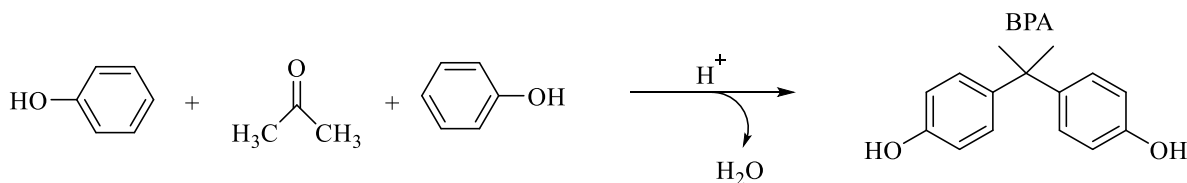


Figure 2 - Reaction scheme of BPA.

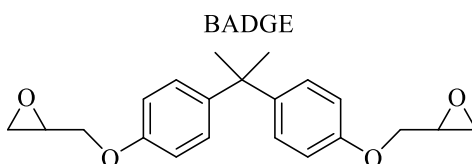
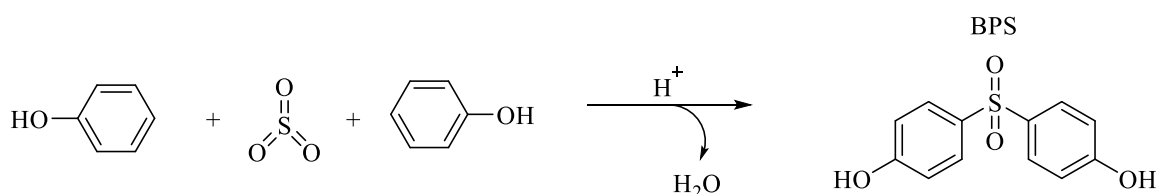


Figure 3 - Scheme of BADGE

However, BPA has for a long time been known as an endocrine disruptor that weakly binds to nuclear estrogen receptors, thereby mimicking the properties of estradiol. BPA has been linked to cause negative effects in reproduction, developmental and metabolic systems in both humans and animals.<sup>5</sup> It has been shown that BPA has leaching properties from the products that it's produced from. The mechanism depends on the product as PC plastics leach more from heat exposure<sup>6,7</sup> while food and drink containers are more susceptible to leaching from mechanical damage and scratching.<sup>8</sup> For all the reason mentioned above, European food safety authority has set a tolerable daily intake of BPA of 0.2 ng/kg bw/day. Furthermore, most producers of baby related merchandise have transitioned to “BPA-free” alternatives.<sup>9</sup> However, the safety of the monomers replacing BPA products has yet to be examined at the depths of the extent of that of BPA. The most popular monomers in question are the closely related BP analogues which are also the main scopes of this thesis; Bisphenol S (BPS) and Bisphenol F (BPF).

The BP analogues are produced by the same acid catalyzed condensation reaction as BPA, while using sulfur trioxide as a reagent for BPS (*Figure 4*) and formaldehyde for BPF (*Figure 5*).



*Figure 4 - Reaction scheme of BPS.*

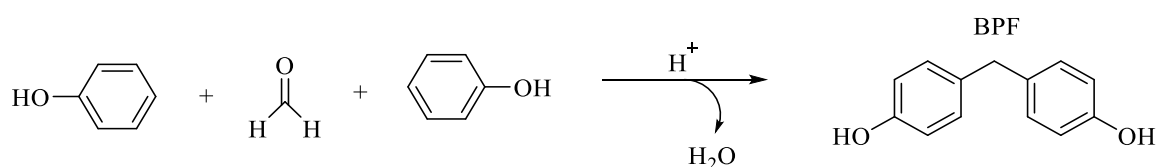


*Figure 5 - Reaction scheme of BPF.*

## 2.2 BP analogues

### 2.2.1 Bisphenol S

The major use of BPS stems from it being used in a replacement for “BPA-free” receipts as a thermal coating for the paper. The most abundant transfer mechanism of these papers to humans are absorption to the skin.<sup>10</sup> BPS is also used as an epoxy resin, much like BADGE, that is used in canned foods and beverages.<sup>11</sup> Therefore, avoiding contamination is almost impossible. A study done in South Korea<sup>12</sup> reported various BP concentrations of the sludge and effluent across domestic, mixed, and industrial WWTPs. The average BPS content of domestic sludge was an order of magnitude lower concentration of 7.1 ng/g dw than the mixed and industrial sludge which was 63 ng/g dw and 74 ng/g dw, respectively. However, the median concentration of the industrial sludge was 30-fold lower than the average, indicating huge outliers of some WWTPs, where the highest sludge concentration was 523 ng/g dw. These WWTPs mainly handled substrate from textile and paper industries and thereby stipulating that these manufacturers are using BPS in their goods. Furthermore, the emission fluxes of BPS content were also studied, where BPS’ average effluent flux in domestic, mixed, and industrial WWTPs

were (9, 95, 68 g/d, respectively) which were 50-fold higher than the BPS content in the sludge that were measured to be 0.2, 1.9, 1.3 g/d, respectively, indicating a 2% removal rate of BPS. Yamazaki performed a study<sup>13</sup> which analyzed the concentration of BP analogues in surface waters of Japan, South Korea, China, and India and found various concentrations across these surface waters ranging from < 10 ng/L across Japan to over 3640 ng/L in Cooum River in India. These ranges of concentrations as well with the knowledge that Cooum River's main supply of pollution is industrial waste<sup>14</sup> support the theory that BPS is more commonly seen from industrial output.

### **2.2.2 Bisphenol F**

In similar fashion to BPA, BPF is industrially used as a finishing coat for furniture and lining and coating for food packaging. Additionally, it is also used as an epoxy sealant for water pipes.<sup>15</sup> Furthermore, a similar epoxy resin of BADGE can also be synthesized. In the same South Korean study<sup>12</sup>, average high levels of BPF were also found in the sludge but stemmed mainly from domestic and mixed WWTP with concentrations of 544 and 699 ng/g dw, respectively. Opposite of BPS' case, however, the median and average concentration was almost identical, pointing to a widespread influent use of BPF. The hypothesis of this observation was mainly due to an increase in epoxy resins used in the domestic water pipes that thereby contain BPF and is slowly leaching out into the influent of the WWTPs. Similarly to BPS' case, the removal of BPF was only 5%. Yamazaki's study et al's study<sup>13</sup> analyzing surface water in Asia found the same results, in which in the regions BPF was detected, the measurements showed where both high and low discrepancies between mean and median. This phenomenon was observed in every country except for in India. Opposite of BPS in this case, it can be concluded that BPF's main use is more of municipal use than industrial use.

### **2.2.3 Endocrinal Disruptive effects of BP analogues**

While the alternative BP analogues have been in circulation for a long time, more studies regarding their ED effects have been performed. Urinary samples of people with no occupational related exposure to BP analogues were tested in the period of 2009-2012. 95%, 78% and 55% of the participants detected exposure of BPA, BPS and BPF respectively.<sup>16</sup>

BPS showed a weak binding of nuclear estrogen receptor of 0.006%, likewise that of BPA. BPS exposure to zebrafish embryo resulted in higher levels of estradiol, reduction of plasma testosterone for males, decreased levels of sperm count and egg production and slower hatching rates for fertilized eggs.<sup>17</sup> It was determined that BPF caused an increase in uterine growth in rats<sup>18, 19</sup>. Furthermore, studies have also shown a decrease in body weight of rats because of exposure to BPF<sup>20, 21</sup>.

Johanna and Bolden<sup>22</sup> made a literature review using several in vitro studies and thereby comparing the hormonal activity of BPS and BPF with that of BPA. The results showed that BPF had similar if not higher estrogenic potency than BPA. BPS had a lower estrogenic potency than BPA. However, while many studies showed that BPS had the same if not lower estrogenic potency as BPA, some studies proclaimed it had little to none. Moreover, a large part of the research had large deviations across both BP analogues, thereby causing a large standard deviation in the proposed hormonal activity. Some of the mechanisms on how the different BP analogues cause estrogenic, developmental, and reproductive effects on organisms may not be exactly mapped out. Although, from their structure alone and the coherent effects that all BP analogues cause, it might not be bold to propose a search for other alternatives for plastic monomers.

## 2.2.4 Biotransformation and biodegradation of BP analogues

The biotransformation of BPA is quite rapid as its half-life is estimated to be 6 hours. The major pathway of BPA biotransformation is the reaction of BPA to BPA-Glucuronide. It has also been shown that BPA has the potential to transform into BPA-Sulfate in the liver, but even there BPA-Glucuronide is the predominant metabolic product (*Figure 6*). The biotransformation of BPA in humans is seen as a deactivation reaction since both the glucuronide and sulfate version of BPA has no estrogenic potency and is excreted in urine.<sup>23</sup> Another study by Kurabayashi et al<sup>24</sup> with rodent subjects uncovers the distinction between the metabolic pathways on humans compared to rodents. It is hypothesized that due to the difference of molecular size capable of biliary elimination between rodents (<375 Daltons) and humans (<500 Daltons), the conjugated BPA – Glucuronide for instance (402 Daltons), BPA-G is more rapidly eliminated for humans. For the case of rodents, 75% of the BPA-G ended up in the fecal matter,<sup>24</sup> while BPA also goes through enterohepatic recycling in rodents, causing the onset removal time to be longer.<sup>23</sup>

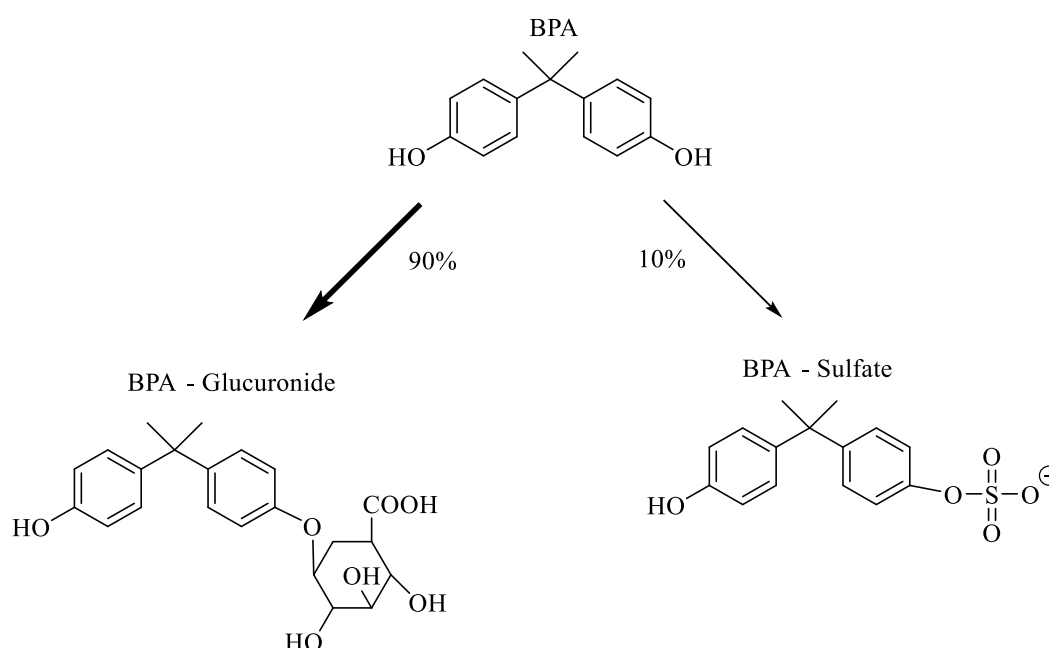


*Figure 6 – The major pathways of biotransformation of BPA.*<sup>23</sup>

The metabolism of BPF is somewhat different that of BPA. The metabolic transformations are identical where BPF is deactivated to form BPF-G and BPF-S respectively. However, while determining the fate of the products on rodents<sup>25</sup>, 80% of these products were excreted in urine. Furthermore, when examining the chemical structures of BPF and BPA, the lack of methyl groups makes BPF slightly smaller (374 Daltons) and more water soluble. The half-life of BPF in the rodents was still higher as for the case of BPA administration, suggesting that BP analogue addition to rats causing enterohepatic recycling.

For BPS, the metabolic pathway mechanism was not researched until a study was performed that uncovered the same mechanism for biotransformation of BPS as with the other BP analogues. BPS-G was yet again the major metabolite. Although BPS-G is of the highest molecular weight of the BP analogues (424 Daltons), a large portion of the metabolic products were found in the urine. In addition, BPS also caused enterohepatic recycling to rodents.

While biotransformation of BP analogues in humans and animals are identical, the case is somewhat different for BP biodegradation. The degradation of BPA was studied<sup>26</sup> under activated sludge (AS) and river water microcosms. Partial degradation (80%) was observed in the time span of 5 days where the lag period was 1 day. Most of the suspected metabolites were mineralized. Other studies have also been conducted and found the major end metabolite to be hydroxybenzaldehyde.<sup>26-28</sup> It should be noted that the other studies used specific strains that could tolerate and easily degrade BPA, but all the studies observed the same non-biodegradable and therefore accumulating metabolites (*Figure 7*).

The main pathways during the study of biodegradation of BPA was found to be hydroxylation (A), methylated hydroxylation (B), hydroxyl elimination (C) and alcohol oxidation (D) although the aforementioned pathway was deemed to accumulate (*Figure 7*).

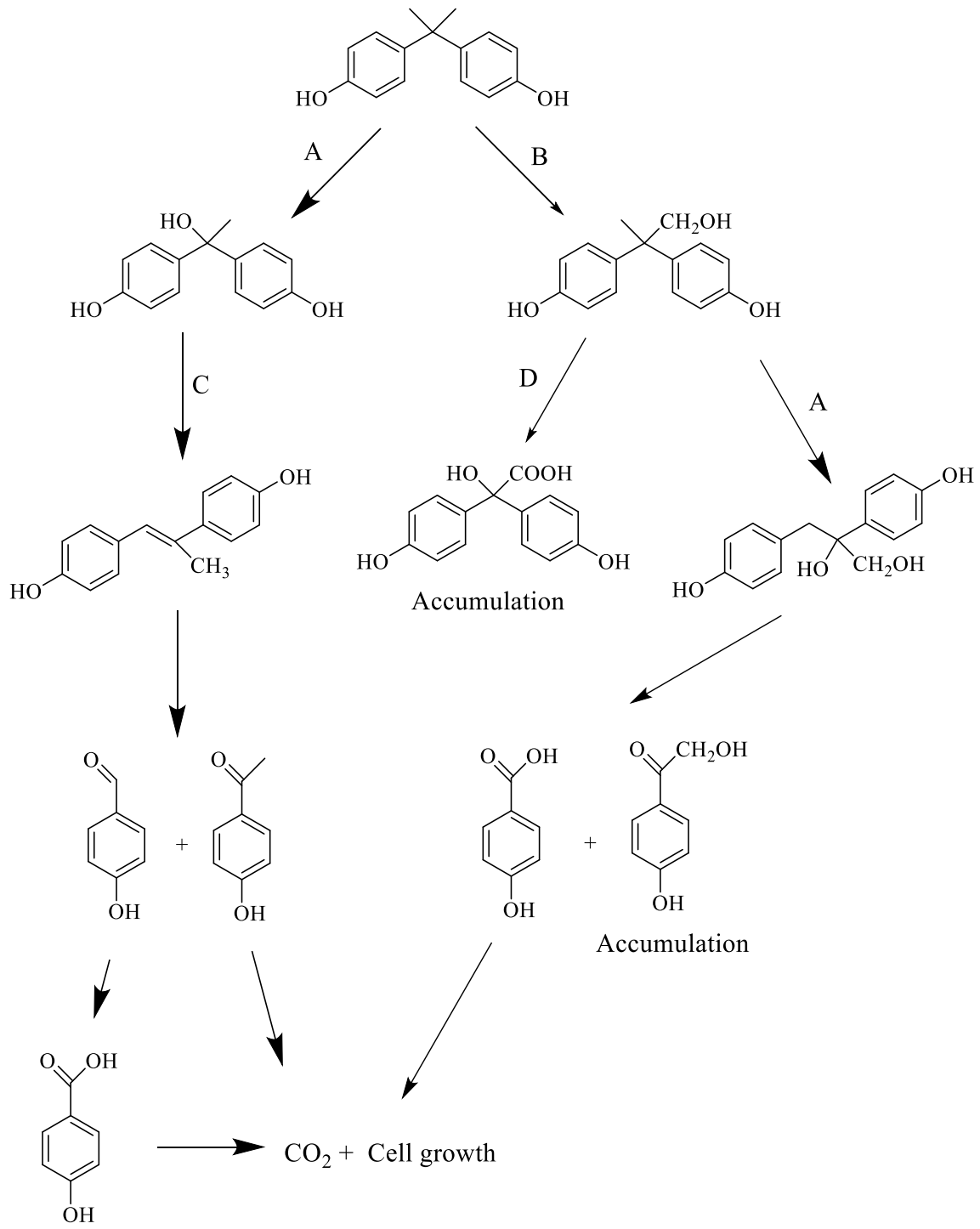


Figure 7 - Proposed bacterial metabolic pathway of BPA<sup>26-28</sup>



The biodegradation of BPF and BPS were analyzed by using biomass from AS.<sup>28</sup> The degradation time of BPF and BPS were 8 and 10 days respectively. However, the lag period and degradation rate decreased significantly when testing larger concentrations. The metabolic pathways of the BPF were mostly hydroxylation in some form while BPS had many different pathways to be degraded. However, all these pathways had different kinetics, possibly contributing to the larger lag time of BPS degradation. The end metabolite for both pathways was determined to be phenol and is easily mineralized.

The main pathways that were observed in the degradation of BPF was aliphatic hydroxylation (A), aromatic hydroxylation (B) and sulphation (C)<sup>29</sup> (Figure 8).

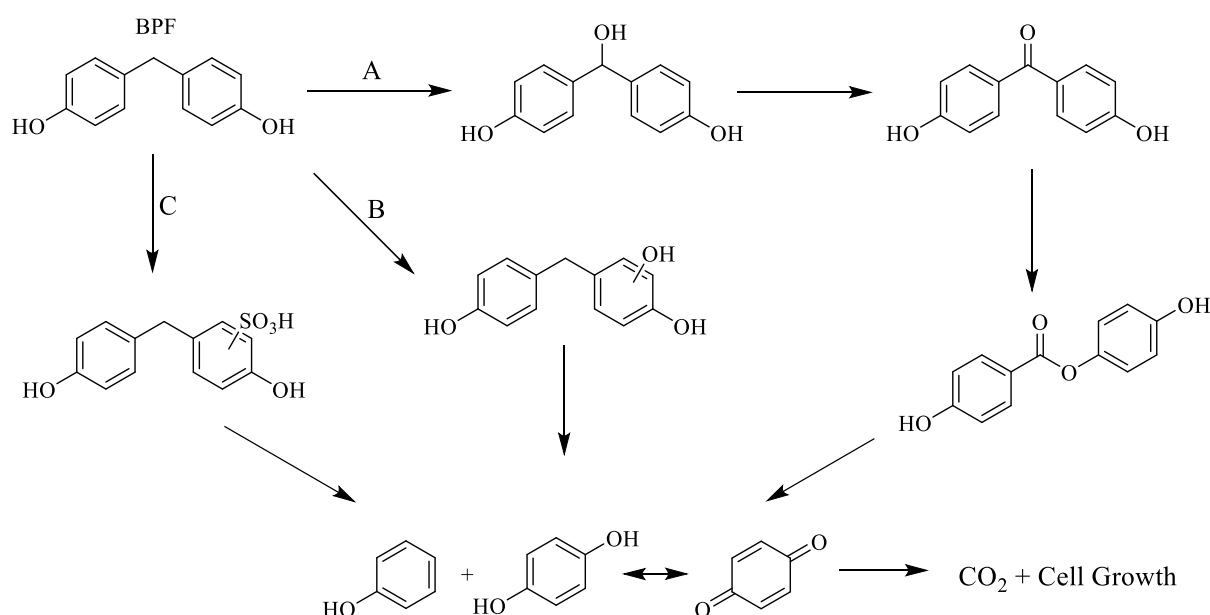


Figure 8 – Proposed bacterial metabolic pathway for BPF<sup>29</sup>

The main pathways that were seen in the degradation of BPS were aromatic hydroxylation (A), aromatic methylation (B), coupling of BPS fractions (C), sulphation (D) and cleavage of S-C bond (E).<sup>29</sup> (Figure 9).

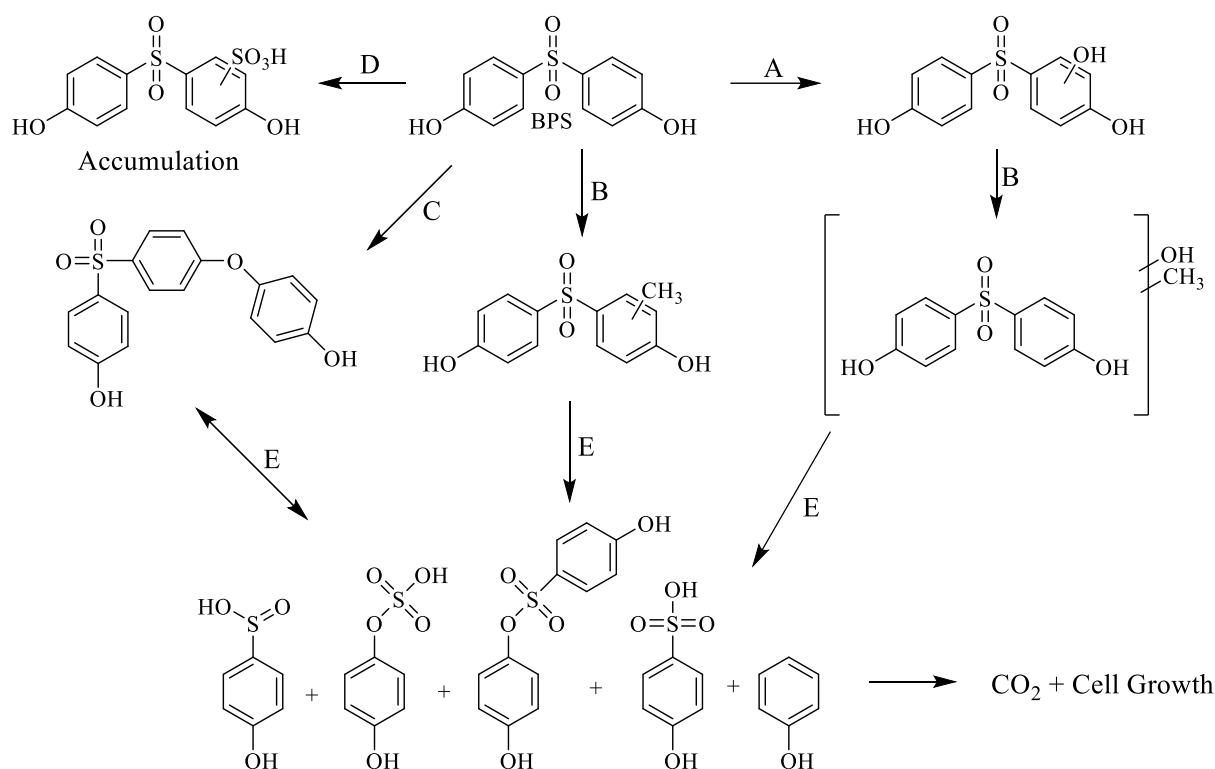


Figure 9 - Proposed bacterial metabolic pathway for BPS<sup>29</sup>

### 2.3 Wastewater Treatment Plants and Activated Sludge System

Wastewater Treatment Plants (WWTPs) are the fundamental facilities in society to help reduce contaminated water from municipalities and industries for the water to be reused or safely discharged into the environment. In recent years, this scope has been broadened as the regulations for not only discharge limits have been stricter, but also the need to recover important nutrients that cause eutrophication. To achieve this, a WWTP consists of multiple stages where the contents of the incoming wastewater is either separated or consumed by mechanical, chemical, or biological processes. These stages are called pre-treatment, primary treatment, secondary treatment, and tertiary treatment. Pre-treatment includes removing bigger and coarser particles that may damage the equipment in the plant. These contaminants are often easily removed by screening which are structures with uniform openings that filters the mentioned particles. The wastewater further moves to primary treatment, in which the particles are removed by settling in a clarifier. The theoretical assumption is that an arbitrary uniform

particle will sink to the sludge collection zone by a critical velocity and all particles that have a slower velocity slower will not be collected. The estimated removal of these particles is dependent on the hydraulic retention time and the area of the basin. Furthermore, incentives such as chemical treatment by coagulation and flocculation are often used to accumulate particles together to stimulate removal efficiency. Here, chemical treatment is also used to remove phosphorous. Secondary treatment consists of biological treatment or often called Activated Sludge treatment (AS). The most common form of AS consists of an aeration tank and a secondary clarifier. Bacteria suspended in the aeration tank consumes the incoming organic matter as substrate. The water traverses through to the clarifier where additional biomass sinks to the bottom and either gets wasted for further treatment such as biogas production or recirculated to the inlet. Other forms of AS systems exist that specialize in removing/recovering nutrients such as nitrogen and phosphorous. The degree of treatment depends on the influent wastewater characteristics and the susceptibility of the receiving water body. In Norway for example, where there is an abundance of water, the treated wastewater can be discharged into the ocean. Disinfection is usually the last unit operation before the effluent is discharged from the plant. The most common unit processes that are applied for disinfection are chlorination, UV disinfection and ozonation.<sup>30</sup>

## **2.4 Activated Sludge Modeling**

In order to understand the effects of the BP analogues in a WWTP, it is important to establish theoretical knowledge to explain how BPs affect the system for which activated sludge models can be utilized. Usually these models govern transportation, biological and chemical processes with many other factors that would be relevant for a WWTP such as hydraulic patterns.<sup>31</sup> However, for the scope of this thesis, we are interested in the oxygen utilization rate (OUR) and the kinetics behind carbon removal and internal storage of substrate by the microorganisms. To establish a realistic model while giving clear explanations on how a complex system like a bioreactor can behave, the activated sludge model No.3 (ASM3) was used, which is based on its predecessor Activated Sludge Model No.1 (ASM1).

### 2.4.1 Activated Sludge Modeling No.1

In ASM1, the processes that are most important for the scope of this thesis is the metabolic activities of heterotrophic bacteria under aerobic conditions. From these activities, aerobic growth and endogenous decay are the most central. During the aerobic growth process, bacteria can only use readily biodegradable substrate ( $S_S$ ) and an electron acceptor, which in this case is dissolved oxygen ( $S_O$ ). Using Monod Kinetics, the change in heterotrophic growth rate can be written as such<sup>32</sup>:

$$\frac{dX_H}{dt} = \hat{\mu}_H \left( \frac{S_S}{K_S + S_S} \right) X_H \quad (1)$$

Where  $\hat{\mu}_H$  is the maximum growth rate ( $d^{-1}$ ) of heterotrophic bacteria and  $K_S$  is the half saturation constant (mg/L) of  $S_S$ .

Substrate intertwines with growth by the heterotrophic biomass yield coefficient ( $Y_H$ ). This explains how much COD gets biosynthesized from one unit of COD. Substrate usually comes in form of  $S_S$ , but also hydrolysable substrate that gets converted to  $S_S$ . Another important substrate part is readily hydrolysable substrate ( $S_H$ ), which to be consumed for growth needs to be hydrolyzed by the microorganisms as and converted to  $S_S$ <sup>33</sup>. The conversion of these types of substrates can be expressed like this:

$$\frac{dS_S}{dt} = \left( -\frac{1}{Y_H} \frac{dX_H}{dt} \right) + \frac{dS_H}{dt} \quad (3)$$

$$\frac{dS_H}{dt} = k_h \left( \frac{S_H/X_H}{K_X + S_H/X_H} \right) X_H \quad (4)$$

$$\frac{dS_S}{dt} = \left[ -\frac{\hat{\mu}_H}{Y_H} \left( \frac{S_S}{K_S + S_S} \right) + k_h \left( \frac{S_H/X_H}{K_X + S_H/X_H} \right) \right] X_H \quad (5)$$

where  $k_h$  is the maximum hydrolysis rate ( $d^{-1}$ ) and  $K_X$  is the half saturation constant (mg/L) for hydrolysis.

Aside from growth, endogenous decay is also an important parameter to consider. During this process, the biomass is decreasing and can be defined as<sup>33</sup>:

$$\frac{dX_H}{dt} = -b_H X_H \quad (6)$$

Where  $b_H$  is the endogenous decay rate ( $d^{-1}$ ).

The general rate of change of heterotrophic biomass can therefore be stated consequently as:

$$\frac{dX_H}{dt} = \left[ \hat{\mu}_H \left( \frac{S_S}{K_S + S_S} \right) - b_H \right] X_H \quad (7)$$

Not all the lost biomass can be mineralized resulting in that remaining part to concentrate into the sludge. This part of the sludge will be regarded as particulate inert organic products ( $X_P$ ) and can be formulated as such<sup>33</sup>:

$$\frac{dX_P}{dt} = -f_{EX} \frac{dX_H}{dt} = -f_{EX} b_H X_H \quad (8)$$

Where  $f_{EX}$  is endogenous residue fraction.

Likewise, substrate that results from  $X_P$  are soluble inert products ( $S_P$ ) that are unable to be converted further.<sup>33</sup> This can be stated likewise as for  $X_P$  as follows:

$$\frac{dS_P}{dt} = -f_{ES} \frac{dX_H}{dt} = -f_{ES} b_H X_H \quad (9)$$

Where  $f_{ES}$  is the fraction of soluble inert products. Both  $f_{EX}$  and  $f_{ES}$  are negative in the middle differential equation due to the property of them increasing as the decays of biomass increases and opposite case for growth. Furthermore,  $f_{EX}$  and  $f_{ES}$  will be categorized as one variable:

$$f_E = f_{EX} + f_{ES} \quad (10)$$

As previously mentioned, oxygen in the form of  $S_O$  is utilized by the microorganisms in every process and its rate of change therefore includes every process and can be done as such<sup>32</sup>:

$$\frac{dS_O}{dt} = \left[ -\frac{1-Y_H}{Y_H} \hat{\mu}_H \left( \frac{S_S}{K_S + S_S} \right) \right] - (1 - f_E) b_H X_H \quad (11)$$

### 2.4.2 Activated Sludge Modeling No.3

That concludes the similarities of ASM1 with ASM3. The significant difference between these models is the ability of ASM3 to simulate internal storage for heterotrophic bacteria. These storage products include but are not limited to polyhydroxyalkanoates (PHA) and glycogen (GLY).<sup>34</sup> One of the reasons for internally storing substrate are in situations where the substrate is not continuously fed to the biomass in which the internal storage products serve as a carbon source during famine periods.<sup>35, 36</sup>

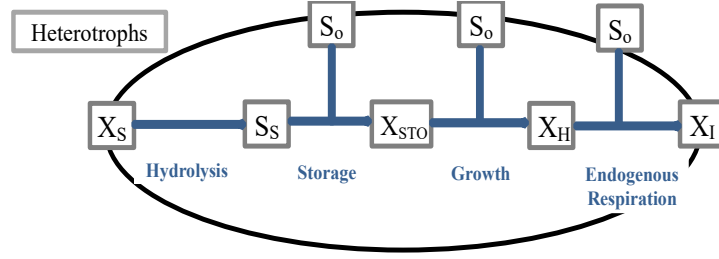


Figure 10 - Diagram of storage process in ASM3<sup>34</sup>

The microorganisms first store  $S_S$  and uses it later for biosynthesis by using  $S_0$  as an energy source (Figure 10). The total amount of  $X_{STO}$  from  $S_S$  are given by the storage yield coefficient ( $Y_{STO}$ ) and are limited by the maximum storage rate ( $k_{STO}$ ).<sup>32</sup> The internal storage products ( $X_{STO}$ ) are coupled together with  $X_H$  during endogenous decay. The change in  $S_S$  during storage and the change in storage during feeding under aerobic conditions can be formulated consequently:

$$\frac{dS_S}{dt} = -k_{STO} \left( \frac{S_S}{K_S + S_S} \right) X_H \quad (12)$$

$$\frac{dX_{STO}}{dt} = Y_{STO} k_{STO} \left( \frac{S_S}{K_S + S_S} \right) X_H \quad (13)$$

$X_{STO}$  is important to consider during growth of heterotrophic biomass due to the microorganisms using the biopolymers as feed during biosynthesis<sup>34</sup>. The change in biomass of storage products could be stated as such:

$$\frac{dX_H}{dt} = \hat{\mu}_H \left( \frac{\frac{X_{STO}}{X_H}}{k_{STO} + \frac{X_{STO}}{X_H}} \right) X_H \quad (14)$$

Consequently, consumption of  $X_{STO}$  is dependent on  $Y_H$  and can be finally written as<sup>32</sup>:

$$\frac{dX_{STO}}{dt} = \frac{\hat{\mu}_H}{Y_H} \left( \frac{\frac{X_{STO}}{X_H}}{k_{STO} + \frac{X_{STO}}{X_H}} \right) X_H \quad (15)$$

The modified condensed matrix of all aerobic equations used in ASM3 can be found (Table 1)

Table 1 - Matrix representation of ASM3

Components →	S <sub>O</sub>	S <sub>S</sub>	S <sub>H1</sub>	S <sub>H2</sub>	X <sub>H</sub>	X <sub>P</sub>	S <sub>P</sub>	X <sub>STO</sub>	Rate Equations
Processes ↓									
Growth of X <sub>H</sub>	$-\frac{1 - Y_H}{Y_H}$	$-\frac{1}{Y_H}$			1				$\hat{\mu}_H \left( \frac{S_S}{K_S + S_S} \right) X_H$
Hydrolysis of S <sub>H1</sub>		1	-1						$k_{h1} \left( \frac{S_{H1}/X_H}{K_X + S_{H1}/X_H} \right) X_H$
Storage of PHAs	$-(1 - Y_{STO})$	-1						Y <sub>STO</sub>	$k_{STO} \left( \frac{S_S}{K_{STO} + S_S} \right) X_H$
Growth on PHAs	$-\frac{1 - Y_H}{Y_H}$				1			$-\frac{1}{Y_H}$	$\hat{\mu}_{STO} X_{STO}$
Decay of X <sub>H</sub>	$-(1 - f_E)$				-1	f <sub>EX</sub>	f <sub>ES</sub>		b <sub>H</sub> X <sub>H</sub>
Parameters	O <sub>2</sub>	COD	COD	COD	Cell COD	COD	COD	COD	

### 2.4.3 Respirometry and Oxygen Utilization Rate (OUR)

Respirometry is the quantification of rate of used dissolved oxygen by microorganisms in activated sludge and is measured by the rate of removed oxygen by volume and time. Respirometry is therefore crucial when observing substrate consumption by bacteria. Furthermore, it is key when determining the effects of toxic pollutants and their inhibiting properties for the microorganisms.<sup>37</sup> This is achieved by measuring the OUR of the system where OUR is the amount of dissolved oxygen used per rate of time.

## 2.5 Enzyme inhibition

In order for the microorganisms to degrade the substrate and use it for growth, they use specific enzymes for particular chemical reactions such as hydrolysis for complex substrate or polymerization for storage. However, due to interferences from inhibitors, which have the ability to disrupt the chemical reactions of the enzymes and the substrate, the efficiency and activity of these enzymes are affected. Depending on which inhibitors in question, there are also different mechanisms in how the enzymes are being disrupted.

### 2.5.1 Competitive inhibition

Competitive inhibition occurs when the inhibitor has a weak affinity to the substrate-specific binding site. The inhibitor binds to the active site of the enzyme, thereby making the enzyme non-reactive. Following is a scheme that can illustrate the mechanism of competitive inhibition:



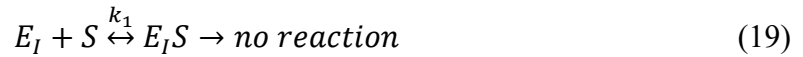
When the inhibitor (I) binds to the active enzyme (E), the available active enzymes in the system decreases. For the biomass, this increases the half saturation constants ( $K_S$  and  $K_X$ , respectively). To combat competitive inhibition, increasing the substrate available will increase the probability of substrate binding to the active enzyme instead of the inhibitor.

### 2.5.2 Non-competitive inhibition

Non-competitive inhibition refers to inhibitors which do not bind directly to the active binding site of the enzyme. On the contrary, the inhibitor binds first on the allosteric binding site of the



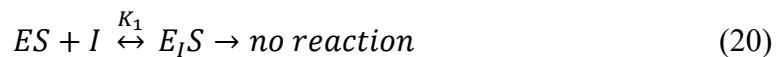
enzyme. The substrate then binds to the active site, but the enzyme cannot proceed to make the desired product. Non-competitive inhibition can be schemed as such:



In the system, where enzymes coupled with allosterically bound inhibitors ( $E_I$ ) cannot proceed to make the desired product of the reaction, the maximum growth rate of the biomass are reduced.

### 2.5.3 Un-competitive inhibition

Much like non-competitive inhibition, the inhibitor binds to the allosteric site of the enzyme. The difference is that the inhibitor binds after the substrate has been bound to the enzyme active site.



The concentration of bound substrate to enzyme (ES) decreases as the inhibitor binds to the enzyme to form ( $E_I S$ ). The formation equilibrium of E and ES shifts, making the concentration of available substrate low, thereby decreasing the half saturation of the reaction. Also, due to the product efficiency being slowed down by  $E_I S$ , the reaction rate is equally reduced.<sup>32</sup>

### 3. Materials and Methods

#### 3.1 Reactor Setup and Operations

A 10L sequencing batch reactor was set up using the seed sludge taken from IVAR SNJ Mekjarvik (Stavanger, Norway). The reactor was operated at a sludge retention time (SRT) of 10 days and a hydraulic retention time of 24 hours. The reactor was fed with a peptone mixture as carbon source. Additionally, Sol A was added as a macronutrient and phosphate buffer (Table 2). After sludge wastage (1 L each day), the reactor was left for settling for 1 h. At the end of the settling phase the reactor was emptied until 2 L and filled with feeding solution to 10L. The reactor was then fed with 600 mg COD/L of peptone mixture, where 20 mL of Sol A was added for every 1000 mg COD. The water used to fill the reactor was dechlorinated and neutralized to keep the pH stable.

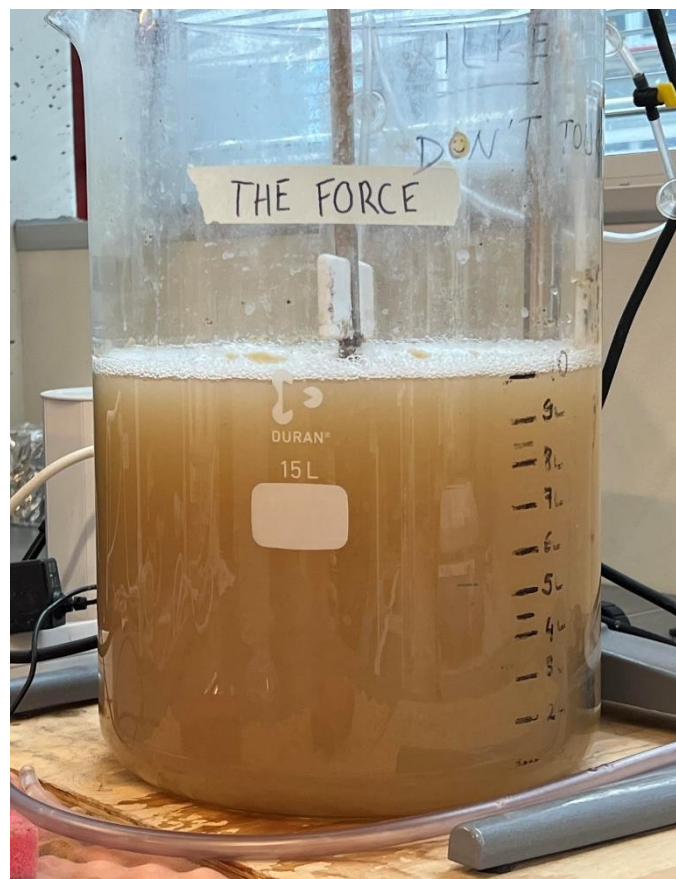


*Figure 11 – Photograph of the control reactor*

In order to test for the chronic impact of the BP analogues on the activated sludge systems, 2.5 L sequencing batch reactors were set up using sludge from the control reactor as chronic seed. Same feeding procedures was applied on the chronic reactors. The feed included peptone mixture, Sol A and relevant BP analogue, and the reactors were exposed to BP's for 30 days. The exposure concentration was chosen as 12 mg/L, as it was mentioned as the highest environmentally relevant concentration in the literature.<sup>38-40</sup>



*Figure 12 – Photograph of the chronic BPA (Left), BPF (Middle) and BPS (Right) reactors*

Table 2- Composition of peptone mixture and Solution A<sup>41</sup>

<b><i>Peptone Mixture</i></b>	
Peptone from Casein	32 g/L
Beef Extract	22 g/L
Urea agar base	6 g/L
NaCl	1.4 g/L
CaCl <sub>2</sub> .2H <sub>2</sub> O	0.8 g/L
MgSO <sub>4</sub> .7 H <sub>2</sub> O	0.4 g/L
K <sub>2</sub> HPO <sub>4</sub>	5.6 g/L
<b><i>Solution A</i></b>	
K <sub>2</sub> HPO <sub>4</sub>	320 g/L
KH <sub>2</sub> PO <sub>4</sub>	160 g/L

## **3.2 Experimental Procedures**

### **3.2.1 Suspended Solids (SS) and Volatile Suspended Solids (VSS)**

Gravimetric analysis was performed in accordance with standard methods 2540D.<sup>42</sup> These were performed two times per week.

### **3.2.2 Chemical Oxygen Demand (COD) and Nitrate Nitrogen (NO<sub>3</sub><sup>-</sup>-N)**

Chemical oxygen demand (COD) was determined by following the procedures of COD test kit 1.14895.001 (Merck). COD tests were performed at the same time as SS and VSS. Nitrate nitrogen (NO<sub>3</sub><sup>-</sup>-N) was determined by following the procedures of NO<sub>3</sub><sup>-</sup>-N test 1.14764.0001 (Merck). Before following the procedures, the wasted sludge was filtered by using a 45 µm syringe filter (Merck Millipore).

### **3.2.3 pH measurement**

pH was determined by using Orion Verastar Pro (Thermo Scientific) according to standard methods 9040C<sup>43</sup>. pH measurements were performed 3-4 times per week.

### 3.2.4 Preparation of BP analogue stock solutions

Each BP analogue stock solutions were made with different concentrations according to their ability to solve in water. The BP analogue (*Table 3*) was added to a beaker filled with distilled water and let to mix for 1 day. The content was transferred to a volumetric flask and the volume was adjusted to 1000 ml. The prepared stock solution was transferred to brown flasks (500 mL) to prevent photodegradation.

*Table 3 – Concentrations of BP analogue stock solutions*

<b>BP analogue</b>	<b>Conc. (mg/L)</b>	<b>COD of 30 mg/L BP</b>
<b>BPA</b>	200	76
<b>BPF</b>	250	72
<b>BPS</b>	500	54

### 3.2.5 Respirometry and Oxygen Utilization Rate (OUR)

Respirometric tests were done using a BM EVO-2 respirometer (Surcis). Oxygen utilization rate graphs were produced for Control, Acute impact and Chronic (Day 30) impact, only BP addition tests.

To test the OUR profile of the reactor, sludge (500 mL) was wasted from the reactor and was let to settle for 1 hour, washed with pH neutral tap water once and settled again for 1 h. The final volume of the Respirometric test reactor was 1 L. During the tests, F/M ratio was kept the same as in the reactors, but in order to prevent oxygen limitation during the test, the sludge and substrate concentrations were halved. The content of the respirometric test reactor was kept the same as the relevant reactor to be tested, however in each test, nitrification inhibitor (Hach, 1 g/L) was added to prevent oxygen utilization due to nitrification. Control test was done without addition of BP analogues to determine the state of the activated sludge without the impact of the BPs. The reactor consisted of sludge, peptone mixture, Sol A, nitrification inhibitor and water. The acute and chronic impact test included relevant BP analogue in addition to the rest.

The only BP addition test was done to determine if there was oxygen utilization due to biodegradation of BPs, in which peptone mixture was not added, and only BP analogue was added as the carbon source. The procedure first started with determining the endogenous decay level of the biomass, where the OUR of the biomass was measured before the addition of the carbon source / inhibitor (peptone mixture / BP analogue). When a stable reading was observed, the baseline of endogenous decay was determined, the test concluded.

After the endogenous decay test, the R test was started. For which, after obtaining a stable OUR profile, the carbon source / inhibitor was added, and the system was observed. Simultaneous measurements of oxygen concentration were taken by the equipment and OUR value for each data point was calculated. During each experiment, COD, NO<sub>3</sub><sup>-</sup> and pH are routinely measured during set intervals. (*Table 4*). When OUR readings reach the baseline of endogenous decay, the test is finished. The OUR experiments were executed at 20°C temperature. However, during the procedures due to fluctuations in temperature, some visible bumps occurred on the OUR profiles, which were then smoothed out in order to get correct modeling results. The original OUR, O<sub>2</sub> and temperature curves for each experiment can be found in Appendix.

*Table 4 – Sampling intervals during an OUR test*

Time (min)	COD	NO <sub>3</sub> <sup>-</sup> -N	pH
-10	X	X	X
2	X		
10	X		
15	X		
30	X		
60	X		
90	X		
180	X		
240	X		
1440	X	X	X

The cells marked with “X” are periods during the experiment where each test is performed. At -10, a sample for SS and VSS are taken. At 2 min, the COD containing content is added (Pep and BP analogue) (to let the mixture homogenize, the time until sample is taken is 2 minutes). Earlier study done by our group<sup>44</sup> showed that the EC50 concentration for BPA was determined to be 30 mg/L, therefore the respirometric tests were done with the addition of 30 mg/L of BP analogue. The volume of BP analogue added varied due to each BP’s stock concentration. To achieve 30 mg/L addition, 60, 120 and 150 mL were added from BPS, BPF and BPA stock solution, respectively. Obtained OUR and COF profile were used for activated sludge modeling. Simultaneous curve fitting for OUR and COD has been done using ASM3. Aquasim was used as the modeling software for this study.

## **4. Results & Discussions**

### **4.1 Analysis of Test Results**

#### **4.1.1 Control Tests**

The control reactor was followed up during the experimental phase. The COD, SS, VS and pH were measured. During the sludge’s acclimation period to peptone mixture, the solids content increased significantly and stabilized at the later stages of operation. The average VSS/SS ratio was deemed to be 81%. The average SS and VSS concentrations after one month of acclimation were  $2900 \pm 290$  mg/L and  $2320 \pm 240$  mg/L, respectively (*Figure 11*). The pH in the reactor was kept at neutral levels. The reactor was fed with 600 mg COD/L peptone mixture every day.

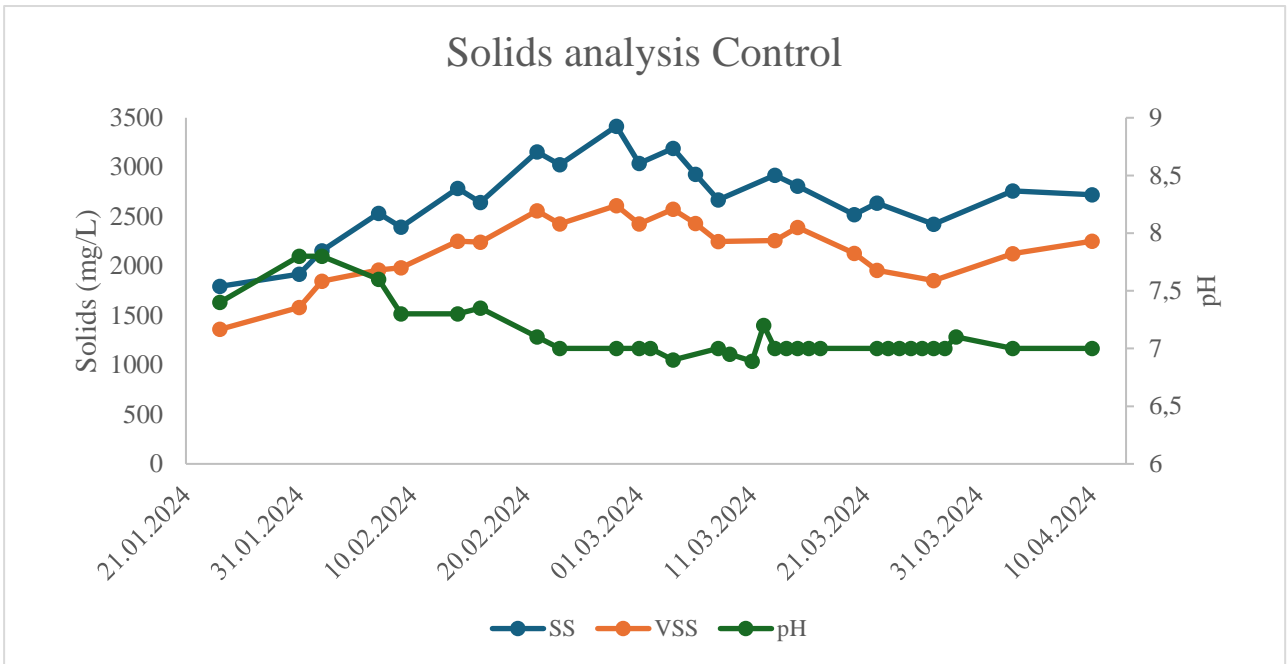


Figure 13 – Solids and pH analysis of the control reactor during operation



Despite some fluctuations in the start of reactor operation, the reactor removed COD at a consistent rate. The average removal during the lifetime operation of the reactor was  $87\% \pm 3\%$  (Figure 14)

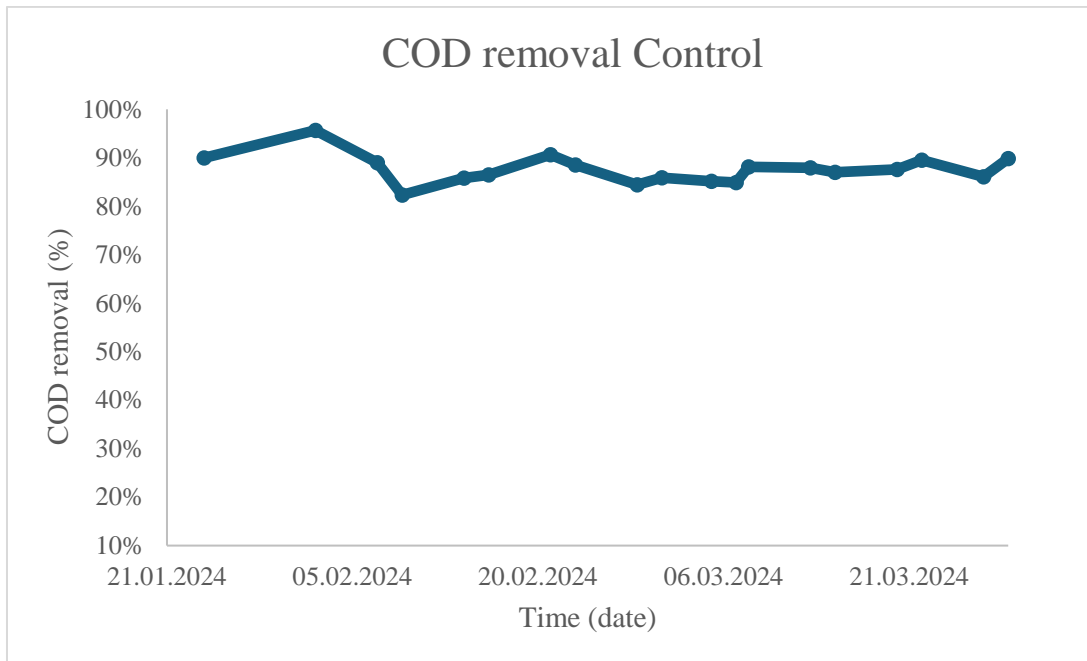


Figure 14 – COD removal efficiency of the control reactor during operation

The control test was done using the sludge taken from the control reactor and feeding the reactor with peptone mixture to determine the baseline of kinetics for organic matter removal without the presence of an inhibitor. The OUR and COD profiles for the control test are given. The OUR graph peaked at  $68.5 \text{ mg O}_2/\text{L.h}$ . Even though the OUR stagnates after 7 hours, the COD profile shows that most of the substrate was consumed after 4 hours. The oxygen that was used for growth was determined to be  $120 \text{ mg O}_2/\text{L.h}$  which converts to a COD consumption of  $300 \text{ mg O}_2/\text{L.h}$  (Figure 15).

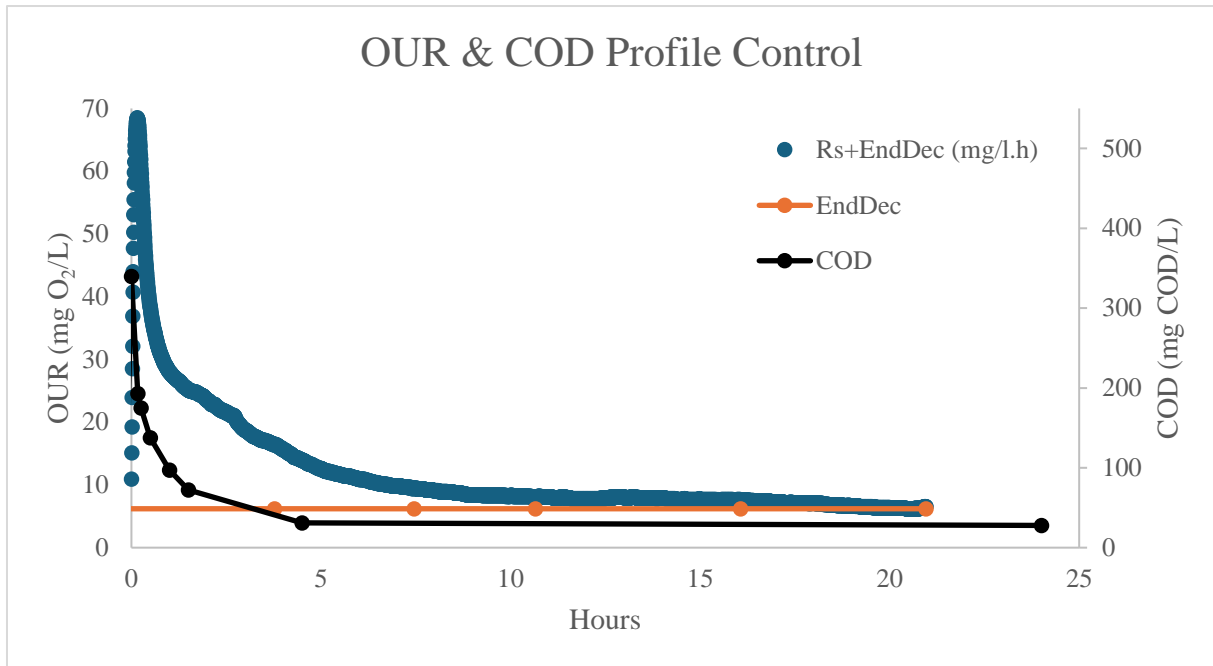


Figure 15 – OUR and COD Profile from Experimental data of Control Reactor

#### 4.1.2 Acute Tests

In order to determine the impact of BP analogues on the activated sludge biomass, which encounter the compound for the first time, acute tests were conducted with 30 mg/L BP analogue additions, which was the previously determined EC<sub>50</sub> concentration for BPA<sup>44</sup>. The peak OUR of BPA was 48.9 mg O<sub>2</sub>/L.h which was the lowest of all BP analogues. Hydrolysis rate was also heavily impacted by BPA addition which can be observed by the stable line in the OUR graph between 5 and 7 hours. The oxygen that the biomass used for growth was calculated to be 112 mg O<sub>2</sub>/L, which gives a COD consumption of 280 mg O<sub>2</sub>/L. The initial COD at the start of the experiment was also the highest. This was due to sampling for the initial COD concentration was performed too early for the system to properly mix, thereby leading to an incorrect COD evaluation. That can be observed by the measurement afterwards (10 min) to be significantly lower. The COD concentration after 24 hours (35 mg O<sub>2</sub>/L) seems to indicate that some of the BPA was degraded. due to the hydrophobicity of BPA, it is plausible that some of the BPA was adsorbed to the sludge<sup>45</sup> (Figure 16).

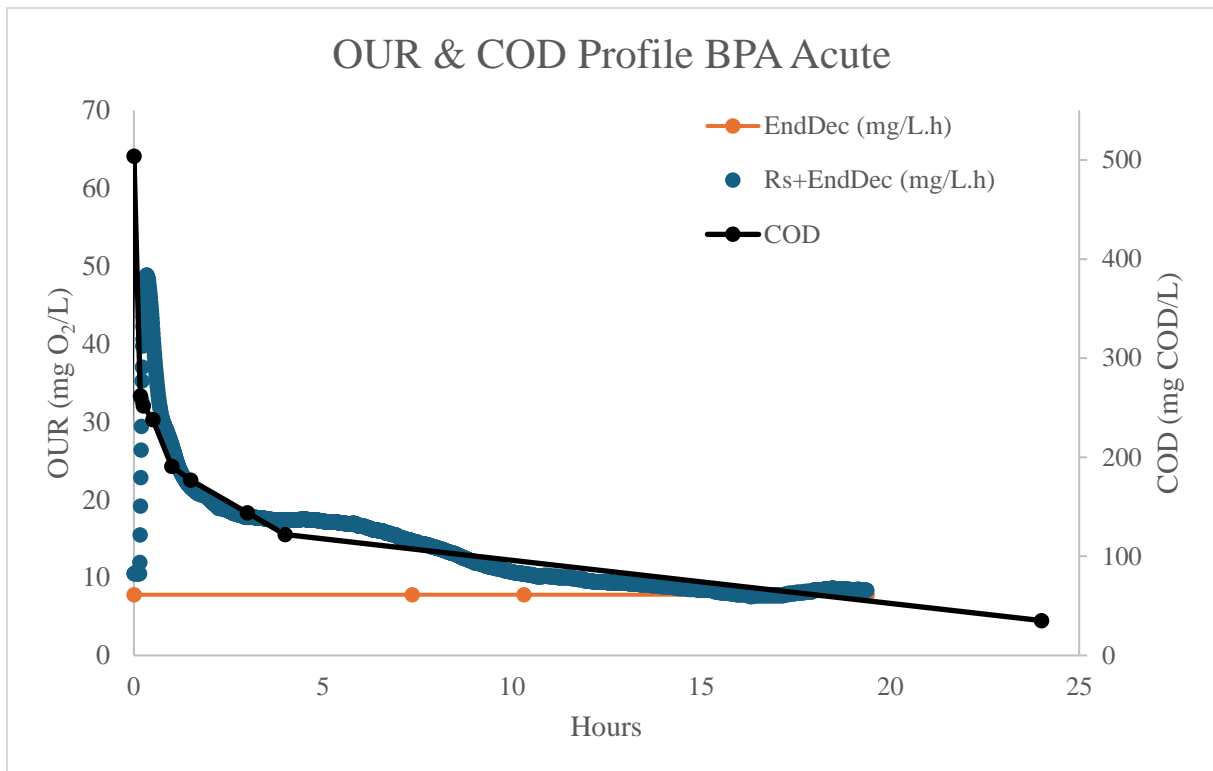


Figure 16 – OUR and COD Profile from Experimental data with BPA addition

The OUR graph of acute BPF addition peaked at 53.3 mg O<sub>2</sub>/L.h, which was slightly less than that of BPS addition. A plateau was visible at this curve as well as it did in the BPS addition indicating that hydrolysis of substrate was impacted also by BPF. The biomass was found to utilize 98 mg O<sub>2</sub>/L or a COD consumption of 245 mg O<sub>2</sub>/L for growth during the test. The COD profile after 24 hours shows a COD concentration of 60 mg/L after 24 hours. Although BPF does not have a lower COD concentration than BPS, the COD level is still high enough to presume there were no biodegradation of BPF. Furthermore, the ability of BPF as BPA to adsorb onto the sludge might also be a factor that resulted in lower effluent COD concentration (Figure 17).

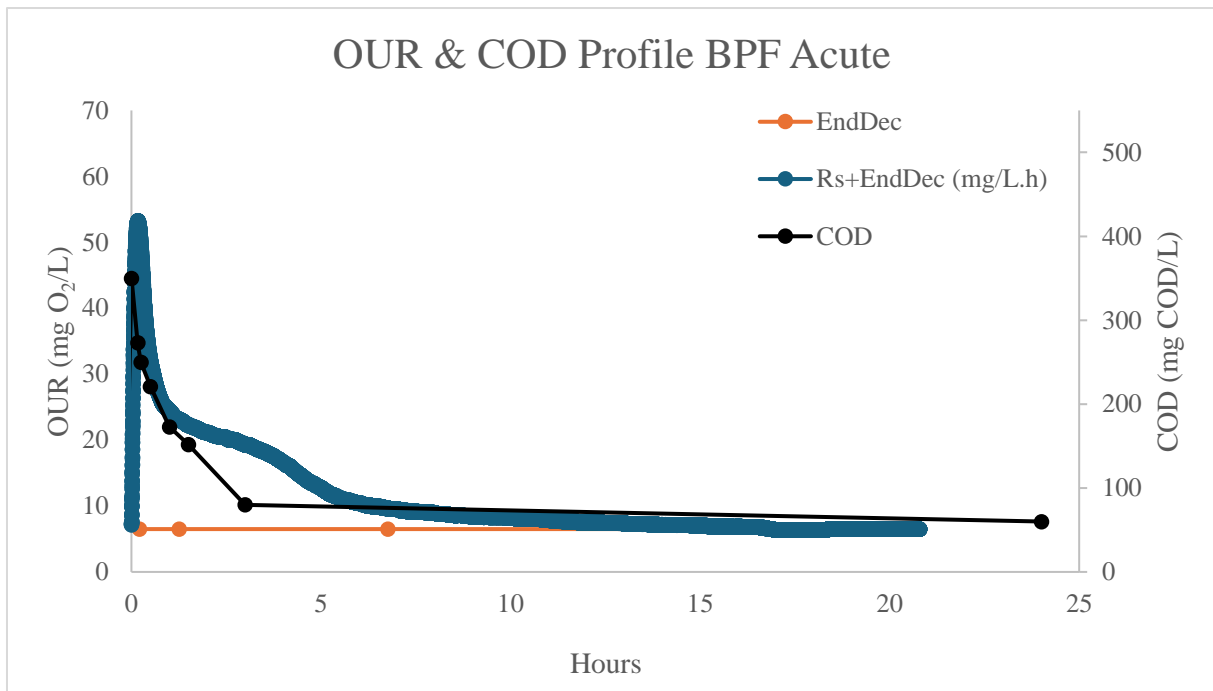


Figure 17 – OUR and COD Profile from Experimental data with BPF addition

The OUR graph of BPS peaked at 58.4 mg O<sub>2</sub>/L.h, which was slightly lower than that of the control test. The shape of the OUR curve also shows that the hydrolysis was impacted as at 4 hours there was seen a noticeable “plateau”. Moreover, the COD concentration is still high after 24 hours (89 mg O<sub>2</sub>/L). This is presumably due to the COD content of the added BPS, thereby indicating the microorganisms were unable to degrade BPS, specifically during the acute exposure. During the test, 118 mg O<sub>2</sub>/L was used for growth. This translates to a COD consumption of 294 mg O<sub>2</sub>/L (Figure 18).

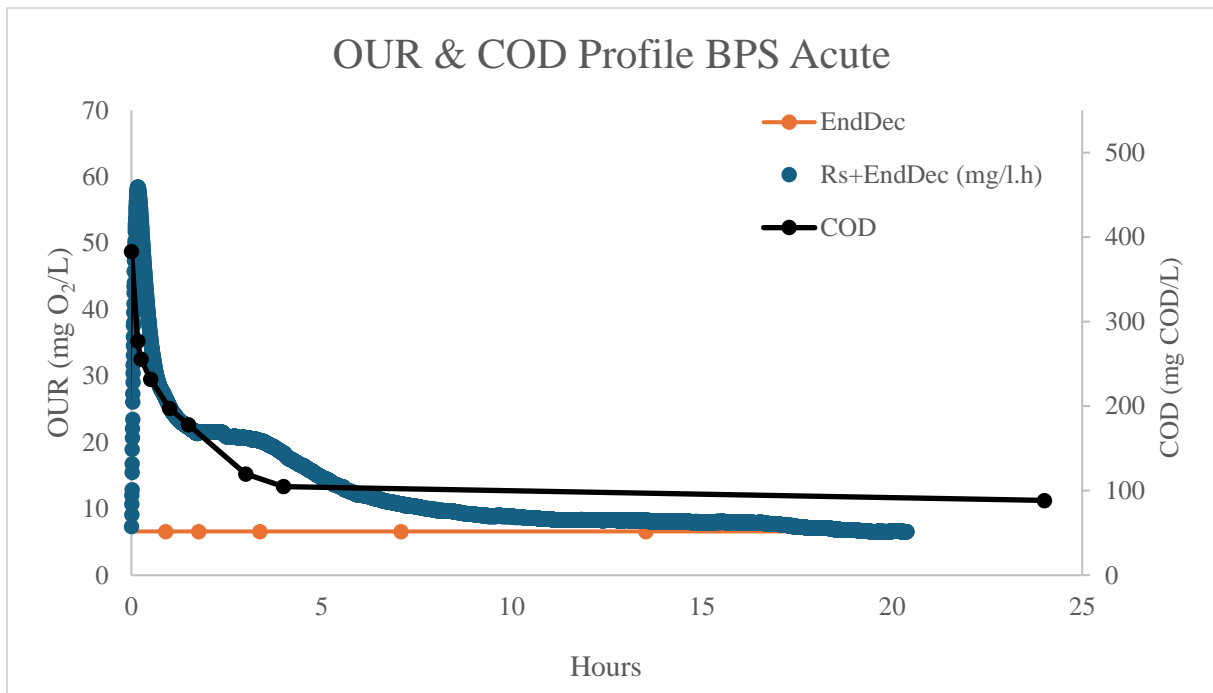


Figure 18 – OUR and COD Profile from Experimental data with BPS addition

#### 4.2 Chronic BP addition

After determining the acute impact of each BP analogue on the activated sludge biomass, chronic reactors were established, which were fed with peptone mixture and respective BP analogues of 12 mg/L concentration characterizing the highest environmentally relevant concentration<sup>38-40</sup>. The chronic reactors were fed for 30 days and at the end of the period, respirometric tests were conducted to determine the impact of EC50 concentration (30 mg/L) on the biomass that had been acclimated to the environmentally relevant concentration-chronic addition before testing the OUR profile. Each reactor was tested based on degradation of their respective BP analogue.

### 4.2.1 Reactor Analysis

A visualization of effects of solids of the reactors before and during the addition of BP analogues are given Figure 19. The measurement immediately after chronic addition, the solids concentration in the chronic reactors dropped significantly. The solids concentration stabilized during the third week but was still lower than that of the control at every point during the chronic phase. The biomass concentration was the most affected by BPA addition, whereas the solids mean concentration dropped almost 30% to the control. BPS and BPF were also largely reduced by 20% and 23%, respectively. The ratio of SS and VSS remained the same (*Figure 19*).

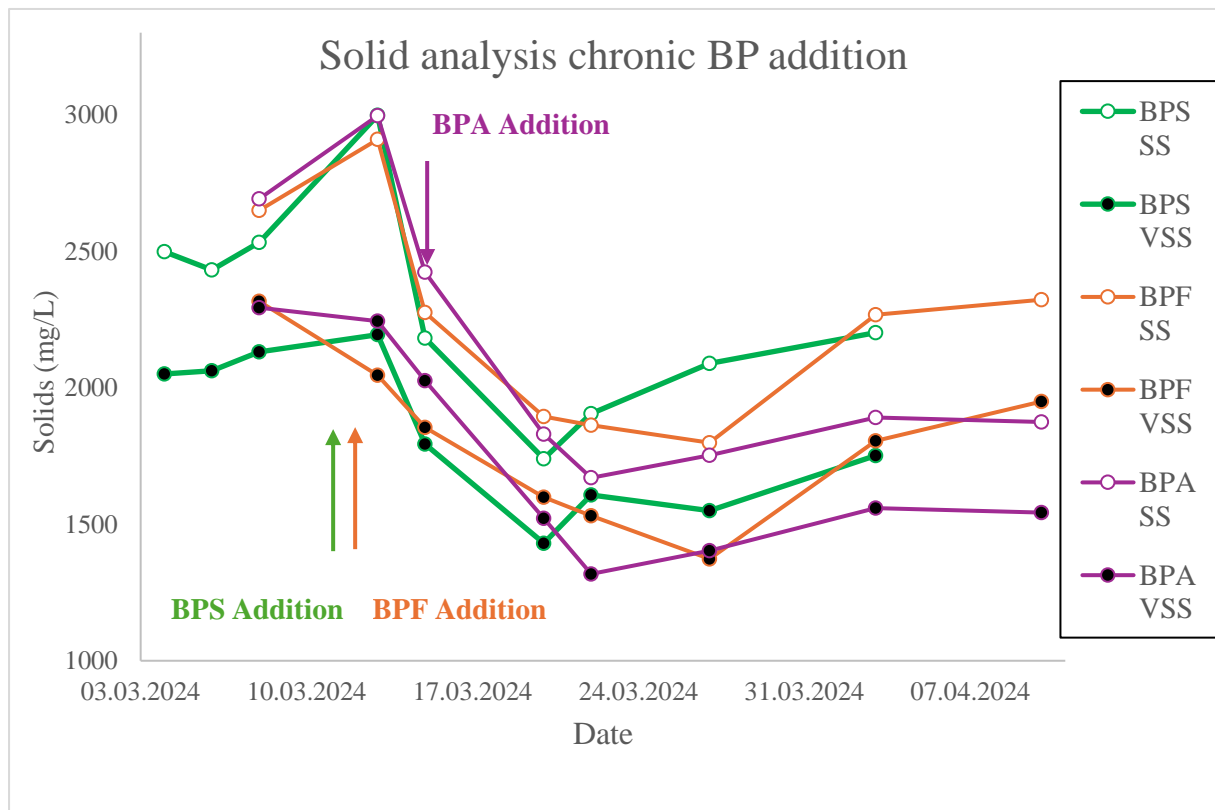


Figure 19 – Solids analysis during chronic BP addition

Figure 20 shows the impact of chronic BP analogue addition on the COD removal of the reactors. It should be noted that COD removal was calculated including the COD addition of the BP analogues. As the solids concentration, the COD removal efficiency dropped drastically compared to the control reactors. At the end of the chronic period, however, BPF and BPS reactors were stabilized and had the same COD removal efficiencies (87%) as the control reactor. This could indicate that the microorganisms acclimated towards the end of the chronic period. The chronic BPA reactor, however, had the lowest COD removal efficiency (80%) (Table 5).

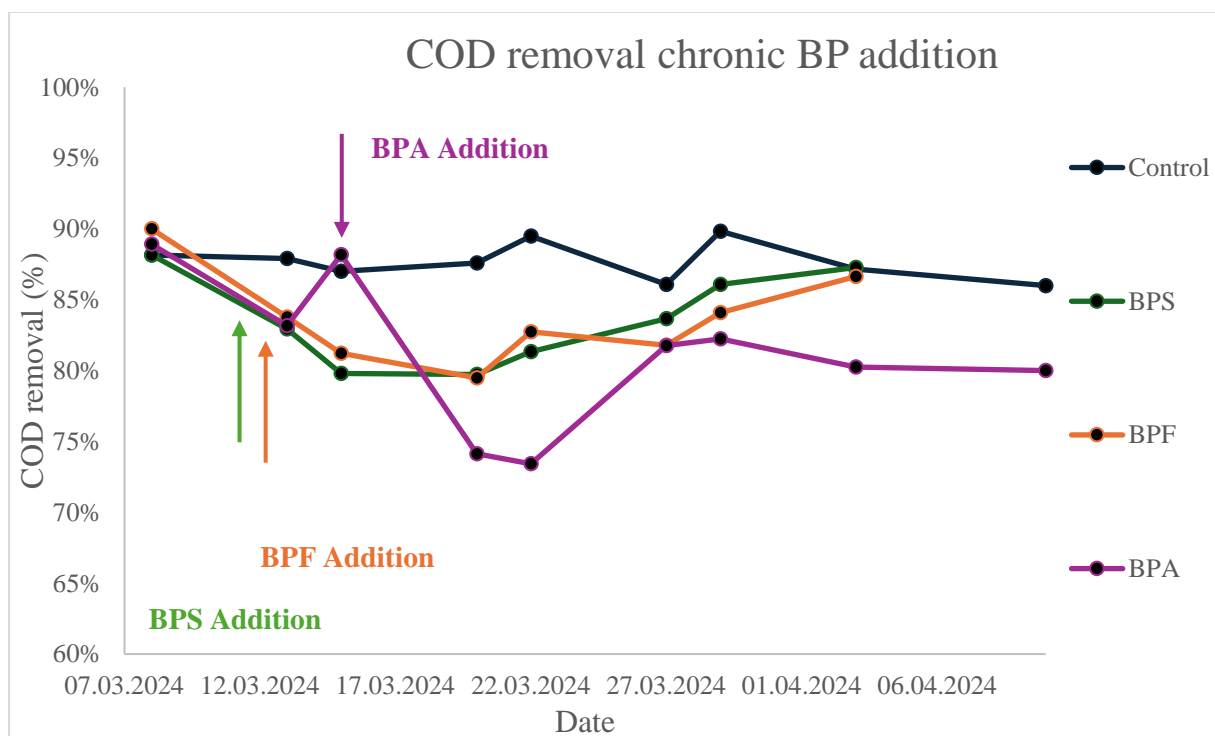


Figure 20 – COD removal during chronic BP addition

Table 5 – Steady state values for solids concentration and COD removal in chronic BP reactors

BP Analogue	Avg. Solids conc. (mg/L) (SS - VSS)	Standard Deviation ( $\pm$ ) (SS - VSS)	Avg. Reduction against Control Reactor (%)	Avg. COD removal (%)	Standard Deviation ( $\pm$ )	Avg. Reduction against Control Reactor (%)
BPA	1910 – 1560	90 - 105	28	80	5	7
BPF	2070 - 1690	240 – 220	23	84	2	4
BPS	2190 – 1720	200 – 150	20	84	3	4

#### 4.2.2 Degradation of BP analogues

In order to determine if the BP analogues were degraded by the activated sludge biomass due to acclimation in the chronic reactors, respirometric tests were performed to determine if there was any oxygen consumption due to BP degradation. During the tests, there were no oxygen consumption observed and thereby no OUR peaks were also observed. Moreover, the COD measurements taken at the end of each experiments shows that remaining COD concentrations (Table 6) were matching the previously determined COD values of reach respective BP (Table 3), indicating that the microorganisms were not able to degrade any mentioned BP.

Table 6 – COD data determined from R-test with only BP addition

BP Analogue	Time (min)	COD (mg COD/L.h)
BPS	-10	<15
	30	60
BPF	-10	<15
	30	65
BPA	-10	<15
	30	73



### 4.2.3 Chronic BP

At the end of 30 days of BP exposure, period respirometric tests were done by adding 30 mg/L BP analogue on the acclimated activated sludge taken from the respective chronic BP reactor. The highest OUR reading measured in the of chronic BPA peaked at 30.8 mg O<sub>2</sub>/L, which an error due to sudden increase in the temperature resulting in a false peak. This peak was not smoothed due to the sensitivity and rapidity of the reactions occurring at this stage. It can be observed that the biomass struggles to utilize the substrate by the linearity of the OUR profile. By calculating the area above the endogenous decay line, the oxygen consumed for growth was found as 105 mg O<sub>2</sub>/L, thereby giving a COD consumption of 261 mg COD/L (Figure 21).

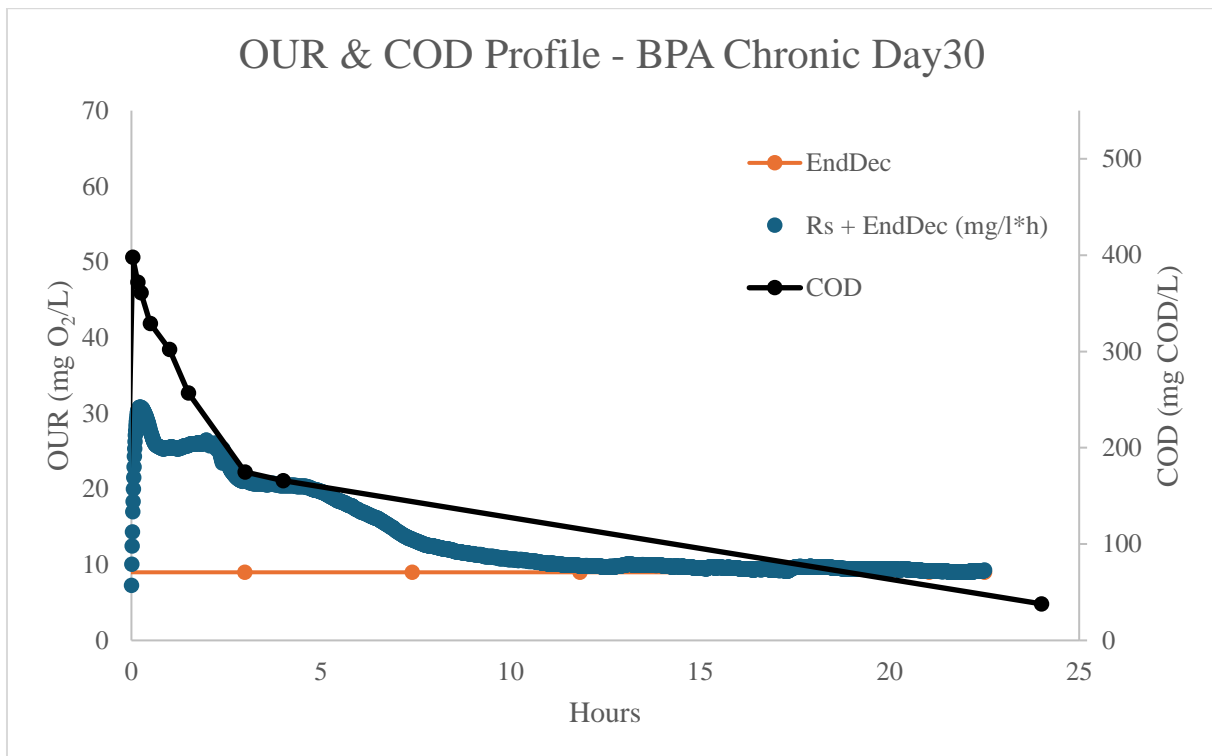
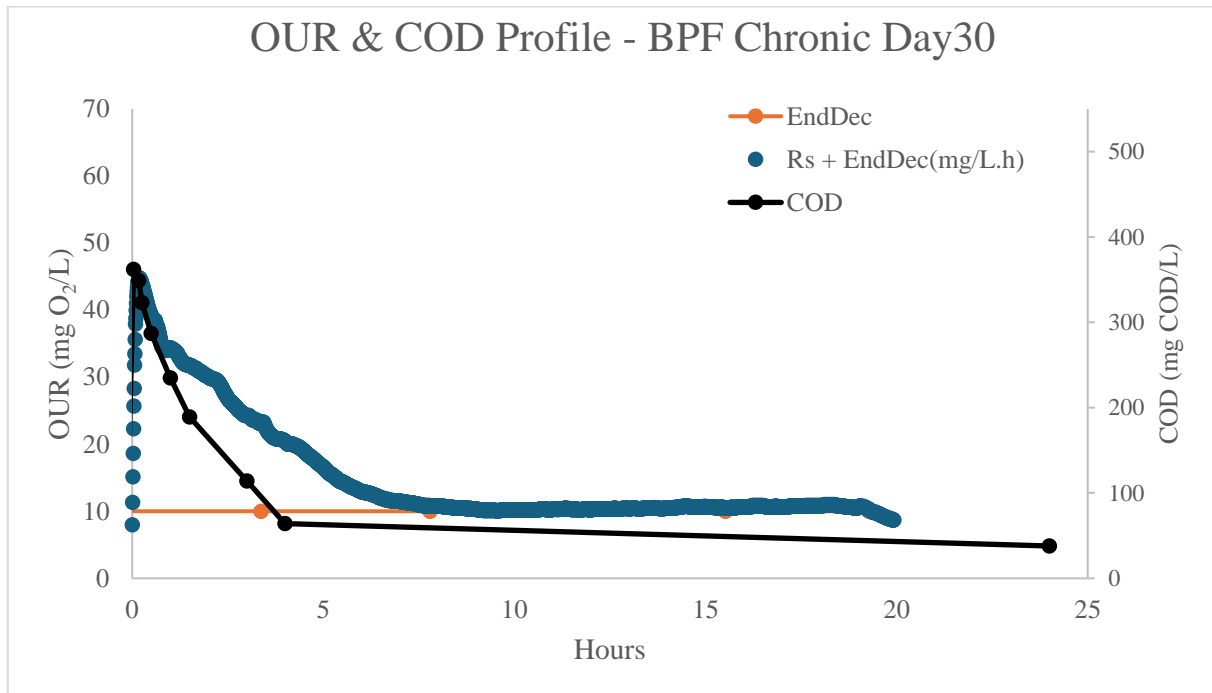


Figure 21 - OUR and COD Profile from Experimental data with chronic BPA addition

The highest OUR value measured in the chronic BPF test was 44.8 mg O<sub>2</sub>/L.h, which was only a slight reduction compared to the acute BPF test and it was the highest peak of all chronic BP's tested. The oxygen utilized by the biomass was calculated as 100 mg O<sub>2</sub>/L, which corresponds to a COD utilization of 249 mg COD/L. The COD reduced rapidly until 4 hours. Likewise, that of BPA, it is possible that a portion of BPF had adsorbed to the sludge and is undetected by the COD readings (*Figure 22*).



*Figure 22 - OUR and COD Profile from Experimental data with BPF addition*

The highest OUR value measured in the chronic BPS test was 28.5 mg O<sub>2</sub>/L.h, which was less than half of the control OUR peak. It can be seen that the biomass used less amounts of oxygen throughout the experiment. By calculation, it was determined that the biomass utilized 116 mg O<sub>2</sub>/L during the experiment, which gives a COD consumption of 289 mg COD/L. The COD after 24 hours was lower (66 mg COD/L) than the measurement during acute testing but not lower than the COD value of added BPS (*Table 3*). From this it can be stated that BPS was not degraded by the biomass (*Figure 23*).

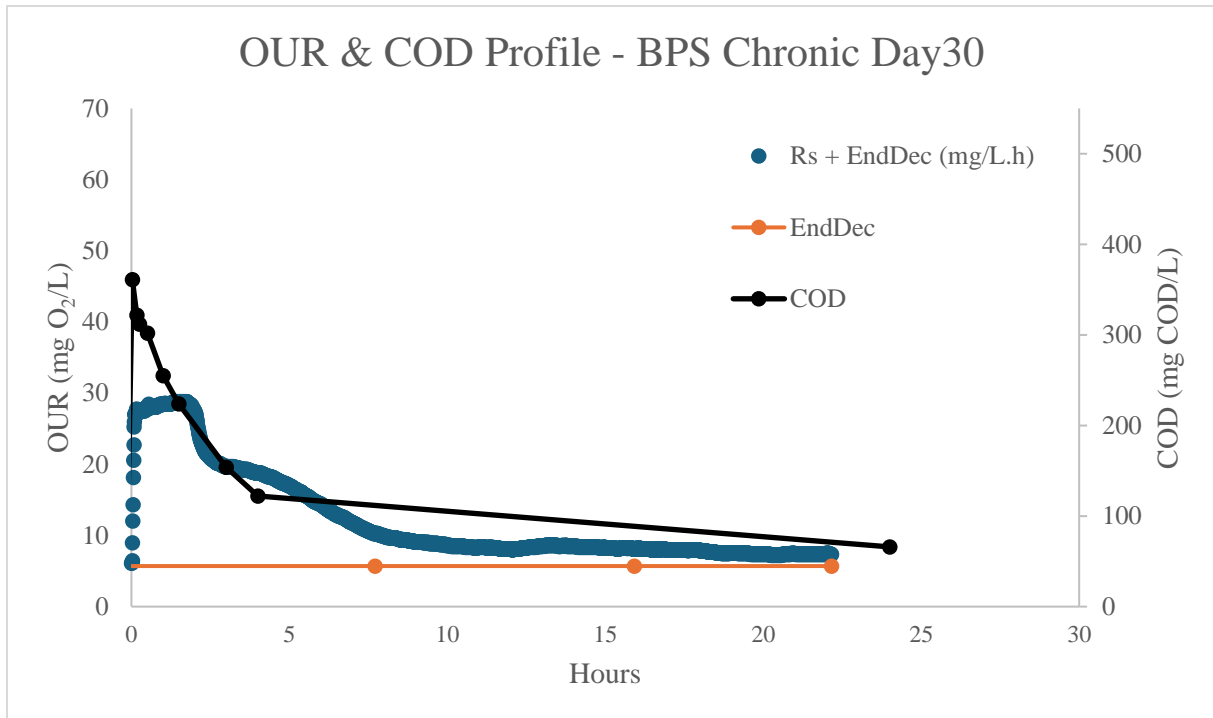


Figure 23 - OUR and COD Profile from Experimental data with BPS addition

### 4.3 Activated Sludge Modelling Results

The results obtained from the experiments were analyzed by activated sludge modelling using Aquasim, where OUR, COD and PHA profiles were fitted to the data. The results of the modelling studies are given in the following chapters.

#### 4.3.1 Control

The OUR profile of the control reactor is the baseline that is being compared with when testing inhibitory effects of BP addition. The modelled OUR and COD profile of the control reactor are given in Figure 24 and the results of model calibration are also given in Table 7. The model calibration showed that the peptone mixture had two COD fractions, namely readily biodegradable and readily hydrolysable COD, which corresponded to 20 and 80% of the added COD, respectively. The OUR model showed that the activity that the biomass largely utilizes storage for substrate removal which later is cleaved out for further growth. Indeed, after 2 hours, the oxygen consumption of the organisms stagnates leaving only stored products to be consumed. The COD profile shows the identical removal of substrate. From the graph,  $S_S$  was consumed or stored after 1.5 hours while  $S_H$  was consumed or stored after 5 hours (Figure 24).

Table 7 – Values of control models determined by model calibration

Model Parameters		Unit	Control
Maximum growth rate for $X_H$	$\hat{\mu}_H$	1/day	3.5
Half saturation constant for growth of $X_H$	$K_S$	mg COD/L	25
Maximum hydrolysis rate for $S_H$	$k_h$	1/day	4.2
Hydrolysis half saturation constant for $S_H$	$K_X$	g COD/g COD	0.14
Maximum storage rate of PHA by $X_H$	$k_{STO}$		2
Half saturation constant for storage of PHA by $X_H$	$K_{STO}$		0.5
Maximum growth rate for $X_H$ on PHA	$\hat{\mu}_{STO}$		1.85
Endogenous decay rate for $X_H$	$b_H$	1/day	0.2
Yield coefficient for $X_H$	$Y_H$	g COD/g COD	0.60
Yield coefficient for storage of PHA	$Y_{STO}$		0.85
Total biomass		mg VSS/L	1164
		mg COD/L	1653
Initial active biomass	$X_H$	mg COD/L	885
Activity		%	54
Initial amount of biodegradable COD	$C_{SI}$	mg COD/L	250
Initial amount of readily biodegradable COD	$S_{SI}$	mg COD/L	50 (20%)
Initial amount of readily hydrolysable COD	$S_H$	mg COD/L	200 (80%)

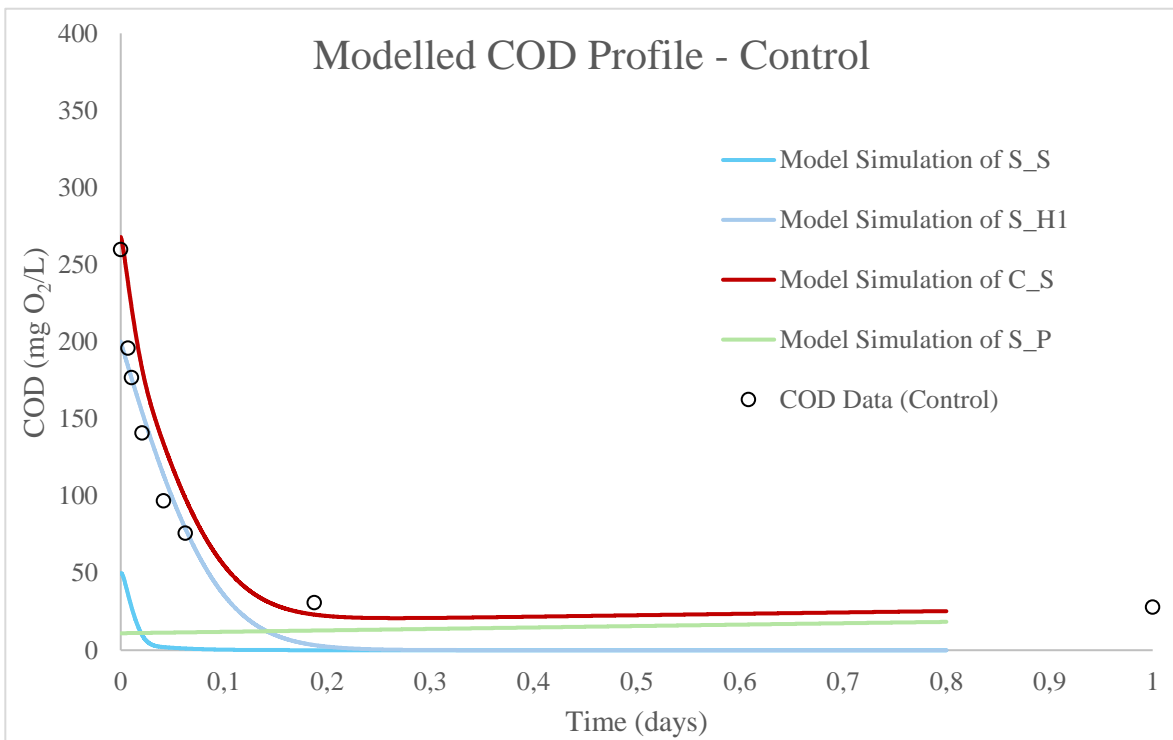
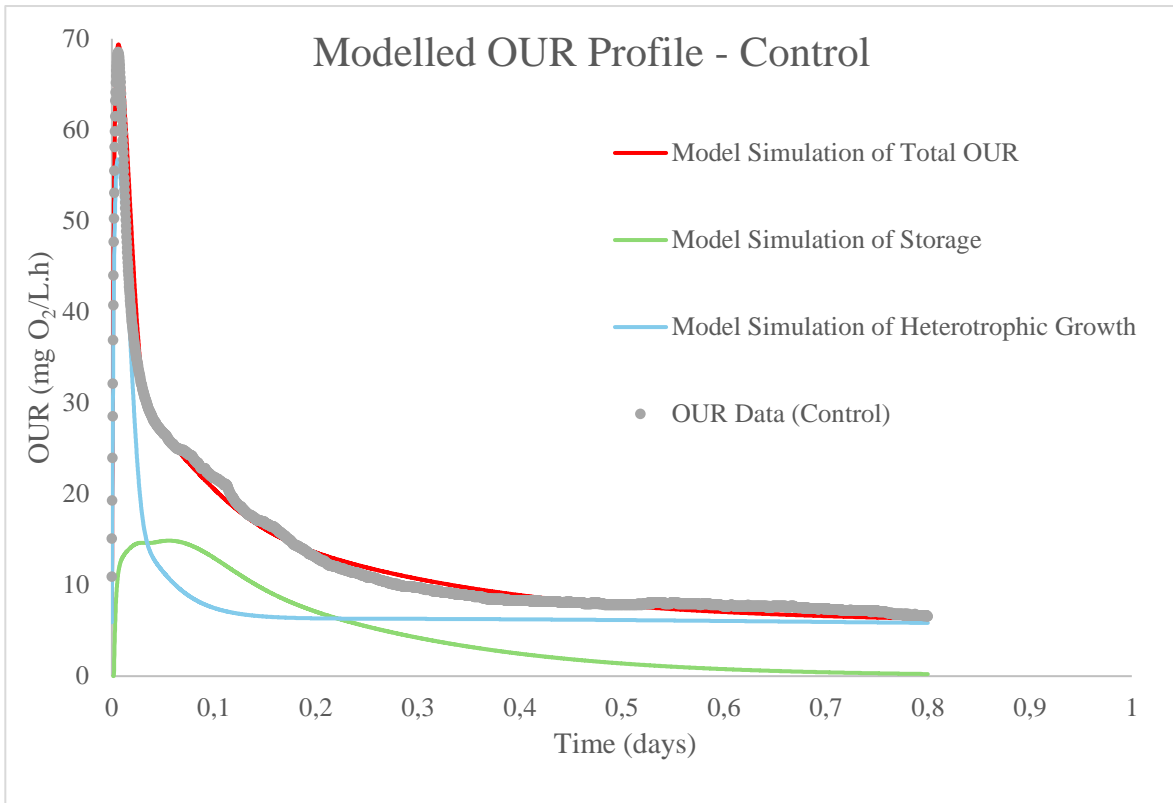


Figure 24 – Modelled OUR (Top) and COD (Bottom) Profiles of control using Aquasim

### 4.3.2 Acute BP

The model calibration for acute BP inhibitions showed that addition of BP analogues had an impact on the half saturation constant for the heterotrophic growth,  $K_S$ , which increased from 25 mg/L in the control experiment to 45, 35 and 30 mg/L for BPA, BPF and BPS additions, respectively. The BP analogues made the substrate less available for the organisms resulting in competitive inhibition.

Looking at the hydrolysis kinetics, it can be seen that both the maximum hydrolysis rate,  $k_H$ , and hydrolysis half saturation constant for hydrolysis,  $K_X$ , are decreased by the addition of BPs, indicating un-competitive inhibition of the hydrolysis reactions. Storage process was also affected the BP addition. Maximum storage rate of PHA,  $k_{STO}$ , decreased for all BP additions, but the half saturation constant for storage of PHA,  $K_{STO}$ , was not affected, indicating non-competitive inhibition of the storage process. Growth on stored PHA was only reduced by BPA and BPF additions. Finally, decay rate was only affected by BPA addition.

Looking at the model simulation of the COD profiles of acute BP additions, it can be seen that additions of BPF and BPS, the removal of readily biodegradable ( $S_S$ ) and readily hydrolysable ( $S_H$ ) substrate was reduced from the control while BPA addition critically reduced the mentioned substrates.

Model simulations for acute BPA, BPF and BPS additions are presented in Figure 25, Figure 26 and Figure 27, respectively.

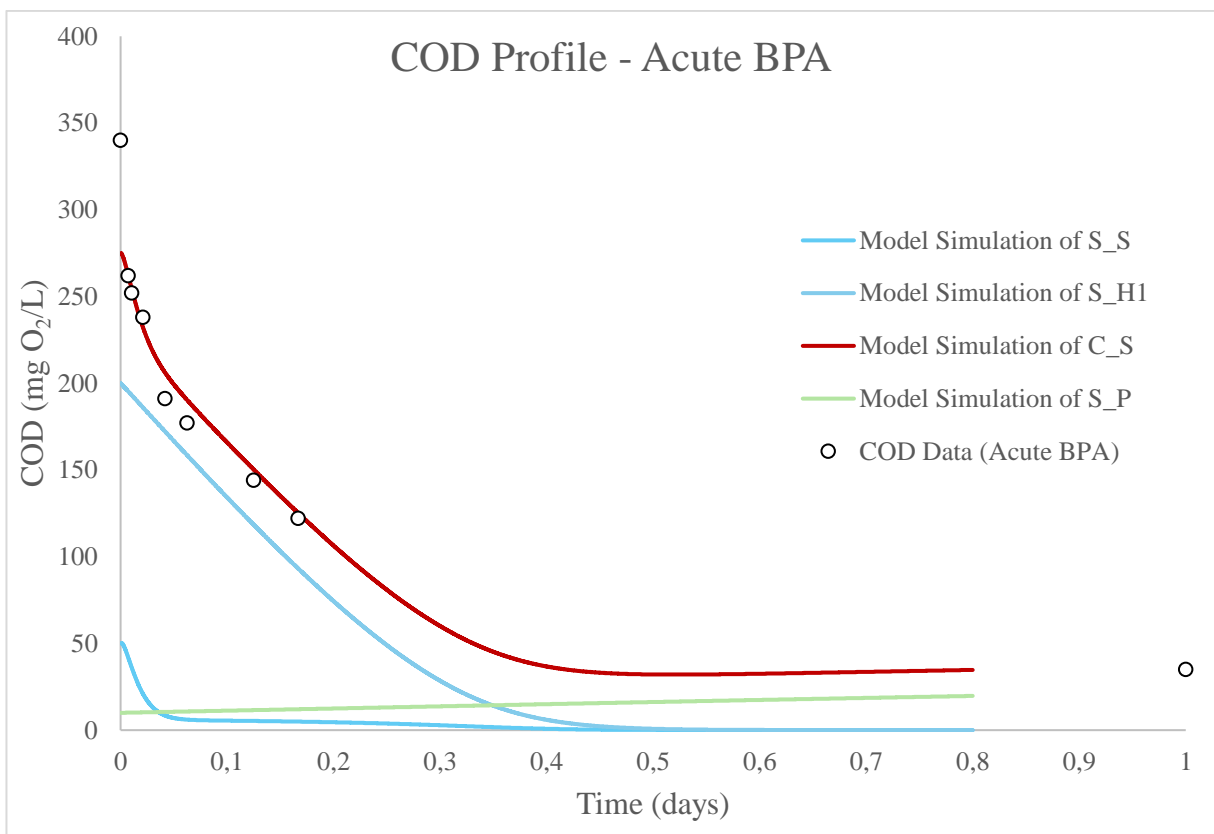
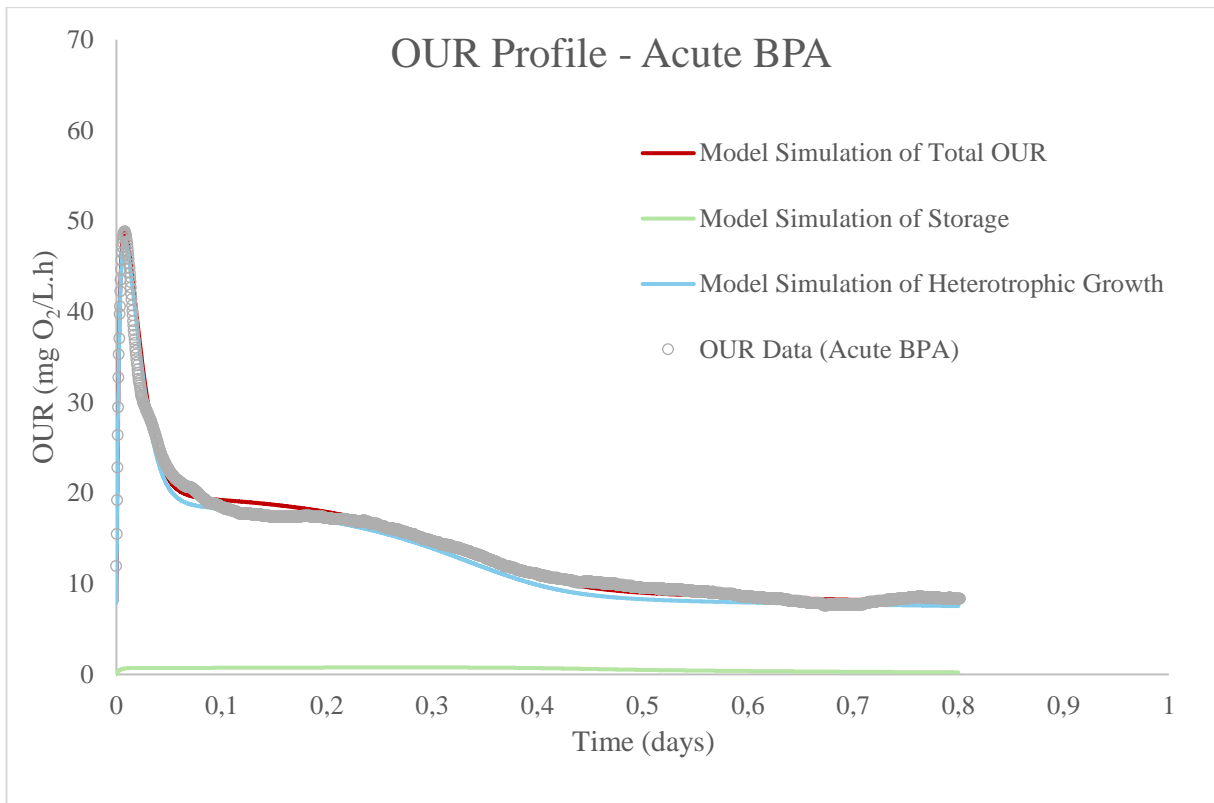


Figure 25 – Model simulation for OUR (Top) and COD (Bottom) Profiles of Acute BPA test

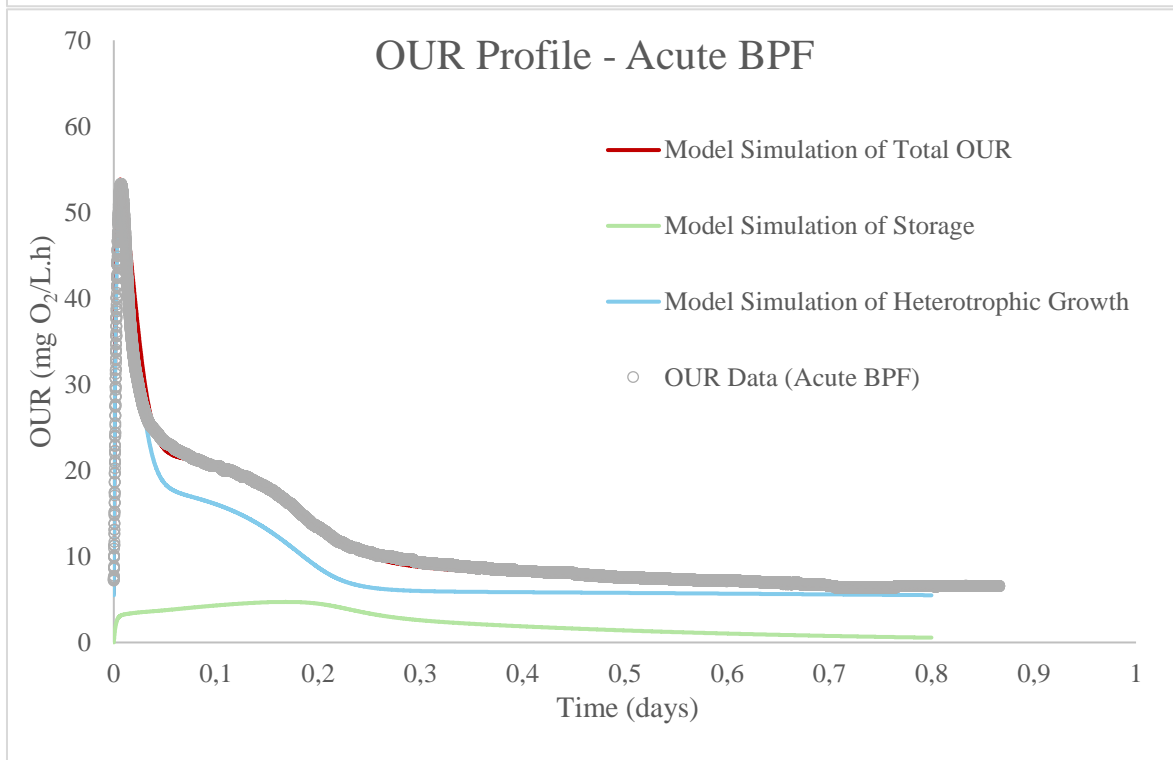
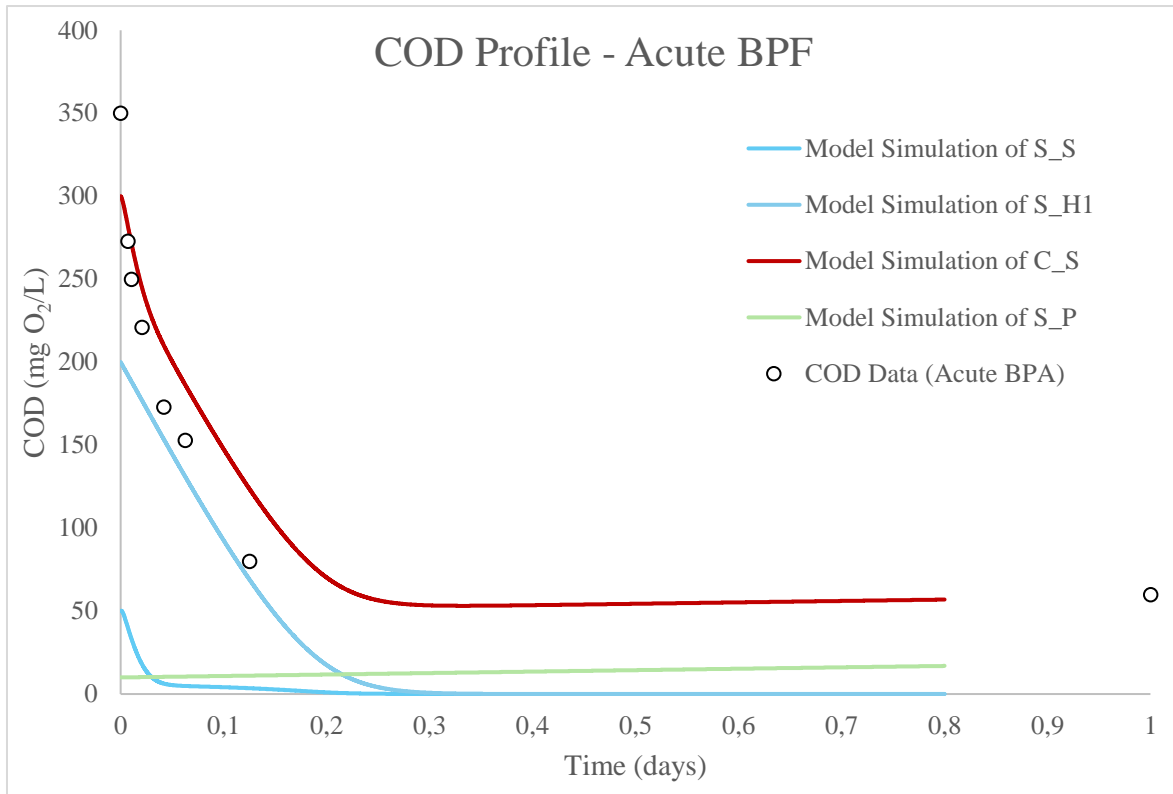


Figure 26 - Model simulation for OUR (Top) and COD (Bottom) Profiles of Acute BPF test



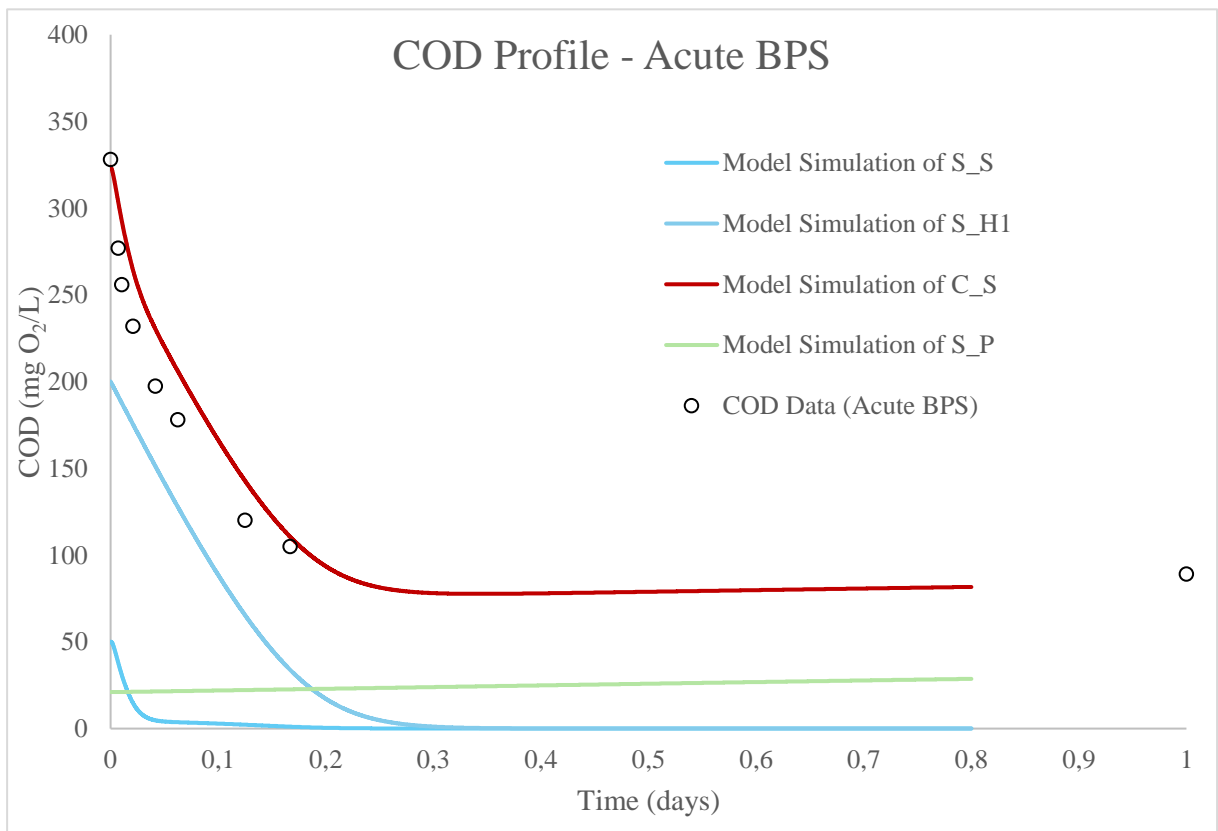
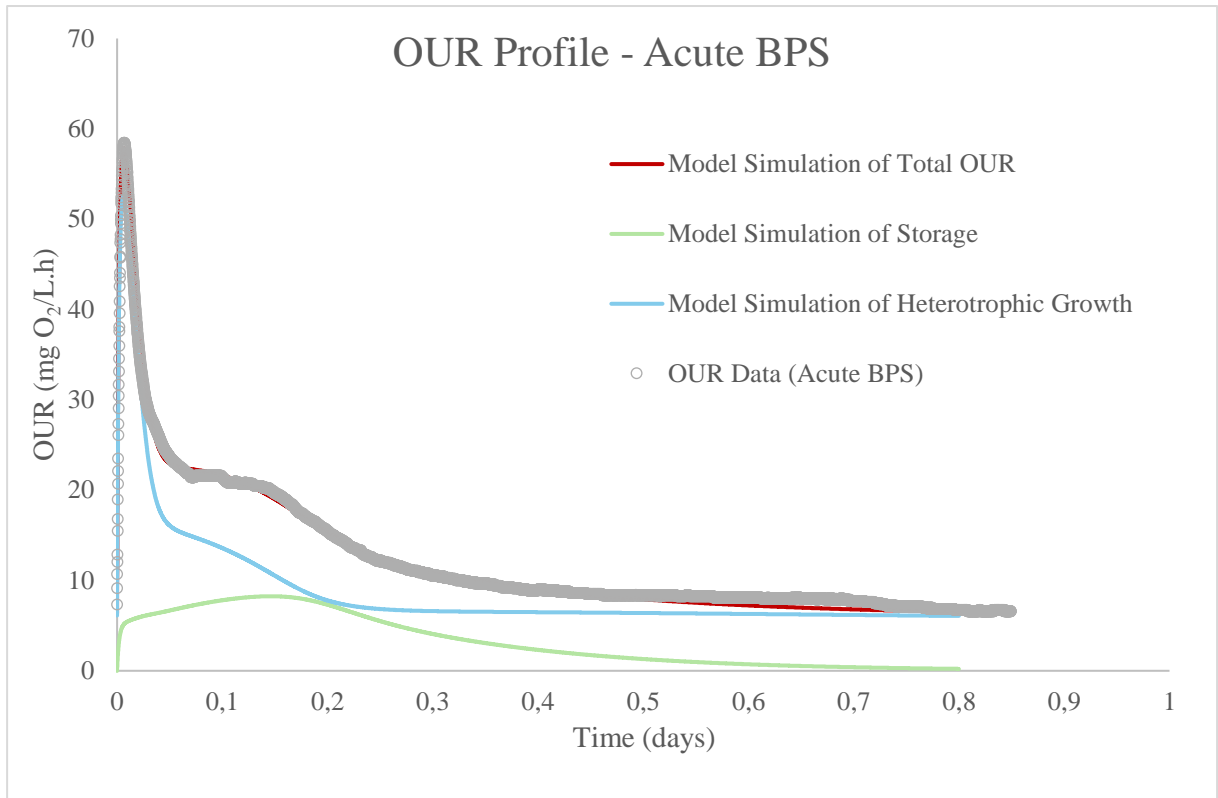


Figure 27 - Model simulation for OUR (Top) and COD (Bottom) Profiles of Acute BPS test

Table 8 - Values of acute models determined by model calibration

Model Parameters	Unit	Control	Acute-BPA	Acute-BPF	Acute-BPS
Maximum growth rate for $X_H$	$\hat{\mu}_H$ 1/day	3.5	3.5	3.5	3.5
Half saturation constant for growth of $X_H$	$K_S$ mg COD/L	25	<b>45</b>	<b>30</b>	<b>35</b>
Maximum hydrolysis rate for $S_H$	$k_h$ 1/day	4.2	<b>0.93</b>	<b>1.6</b>	<b>1.6</b>
Hydrolysis half saturation constant for $S_H$	$K_X$ g COD/g COD	0.14	<b>0.06</b>	<b>0.035</b>	<b>0.053</b>
Maximum storage rate of PHA by $X_H$	$k_{STO}$	2	<b>0.05</b>	<b>0.5</b>	<b>0.7</b>
Half saturation constant for storage of PHA by $X_H$	$K_{STO}$	0.5	0.5	0.5	0.5
Maximum growth rate for $X_H$ on PHA	$\hat{\mu}_{STO}$	1.85	<b>0.75</b>	<b>1</b>	1.85
Endogenous decay rate for $X_H$	$b_H$ 1/day	0.2	<b>0.26</b>	0.2	0.2
Yield coefficient for $X_H$	$Y_H$ g COD/g COD	0.60	0.60	0.60	0.60
Yield coefficient for storage of PHA	$Y_{STO}$	0.85	0.85	0.85	0.85
Total biomass	mg VSS/L	1164	1193	1071	1200
	mg COD/L	1653	1690	1520	1704
Initial active biomass	$X_H$ mg COD/L	885	912	820	920
Activity	%	54	54	54	54
Initial amount of biodegradable COD	$C_{SI}$ mg COD/L	250	250	250	250
Initial amount of readily biodegradable COD	$S_{SI}$ mg COD/L	50 (20%)	50	50	50
Initial amount of readily hydrolysable COD	$S_H$ mg COD/L	200 (80%)	200	200	200

### 4.3 Chronic BP

The model calibration for chronic BP inhibition showed that chronic exposure of BPA had a big impact on the maximum growth rate,  $\hat{\mu}_H$ , which decreased from 3.5 d<sup>-1</sup> to 1.15 d<sup>-1</sup>.  $K_S$  dramatically decreased during the chronic period, changing the inhibition mechanism for growth to un-competitive inhibition. Looking at hydrolysis kinetics, the BPA exposed microorganisms still had severely reduced  $k_H$  and  $K_X$ , suggesting that un-competitive inhibition still was the main cause of inhibition for hydrolysis under BPA exposure. Although, the effect was not nearly as severe as during the acute test, possibly indicating that the biomass had acclimated to BPA exposure. Another case for acclimation of the organisms is that  $k_{STO}$  and  $\hat{\mu}_{STO}$  increased during the chronic period compared to the acute test. However, both parameters were approximately half compared to the control.  $K_{STO}$  remained unchanged, indicating that, for storage, non-competitive mechanism still was the primary mechanism under prolonged BPA exposure. The endogenous decay rate,  $b_H$ , got increased to 0.4 d<sup>-1</sup> compared to the acute BPA and the control test, which had 0.26 and 0.2 d<sup>-1</sup>, respectively. The activity of the chronic biomass was reduced from 54% of the control and the acute test to 47% of that of the chronic BPA (*Table 9*). When looking at the COD profiles of acute and chronic BPA, the consumption rate of  $S_S$  and  $S_H$  had increased, suggesting again that acclimation had occurred during the chronic period (*Figure 28*).

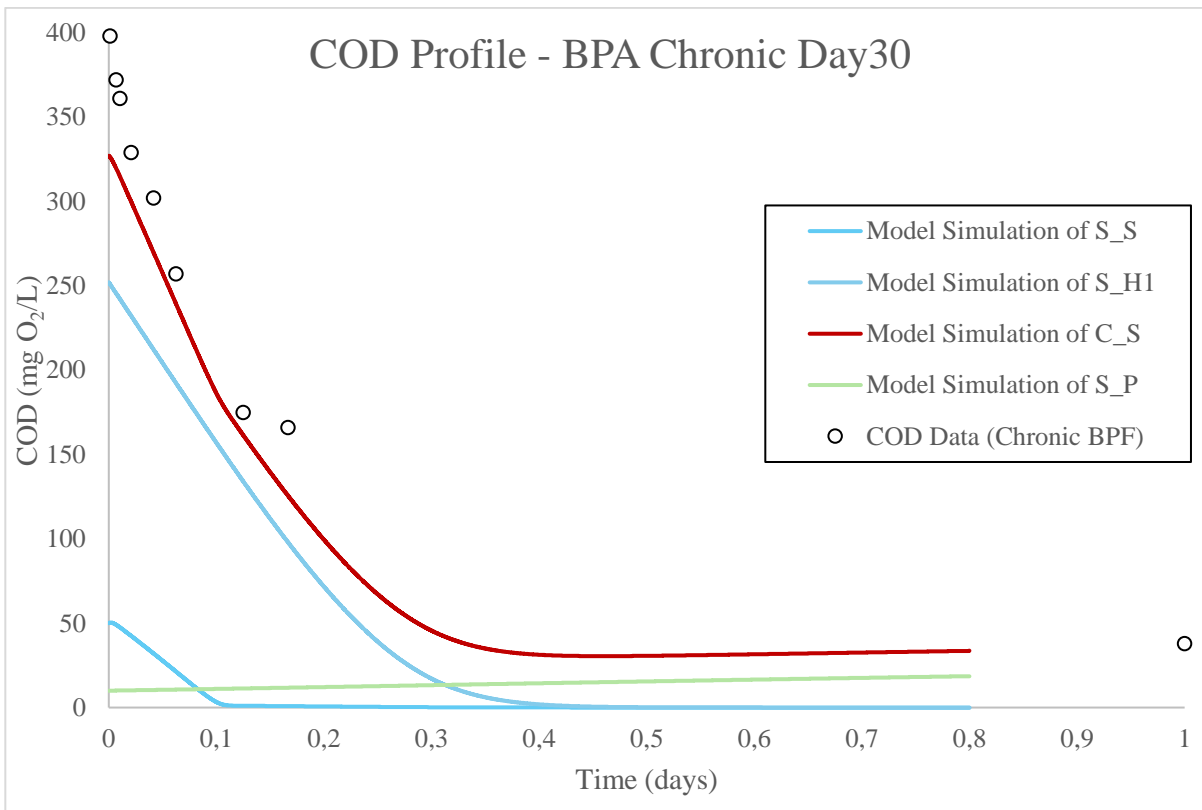
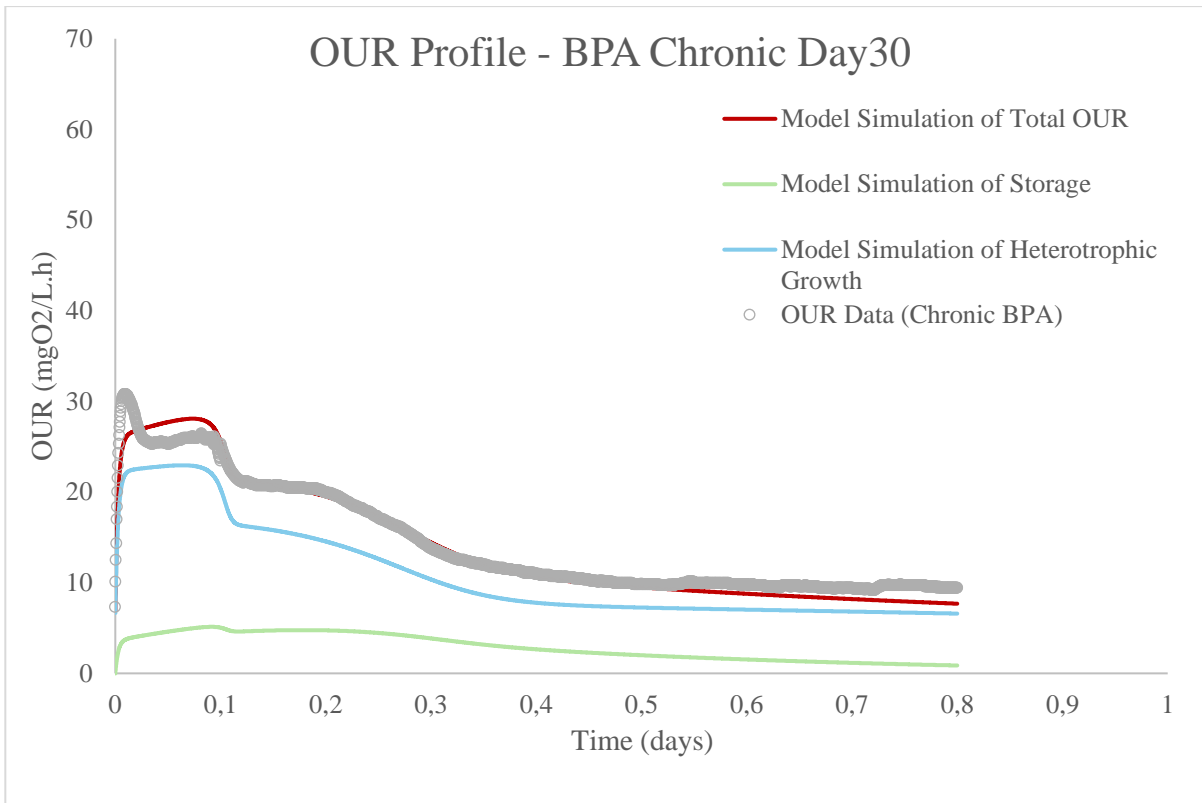


Figure 28 - Model simulation for OUR (Top) and COD (Bottom) Profiles of Chr. BPA test

The model calibration for chronic BP inhibition showed that  $\hat{\mu}_H$  remained unaffected while  $K_S$  was severely impacted at 50 mg COD/L, being double of the control and a large increase from the acute test at 25 and 35 mg COD/L, respectively. BPF made the substrate less available for the organisms and still resulted in competitive inhibition for growth as was the case for the acute test. When observing hydrolysis kinetics, it was found that  $k_H$  and  $K_X$  had increased compared with the acute test, but was still reduced compared with the control test, indicating that the microorganisms also had acclimated during the chronic period. For hydrolysis, this still resulted in un-competitive inhibition for the organisms. For storage on PHA's, both  $k_{STO}$  and  $\hat{\mu}_{STO}$ , was severely reduced during chronic BPF exposure. However, as  $K_{STO}$  was not affected, it suggests that BPF only inhibited the storage of PHA's in a non-competitive fashion. The biomass, when chronically subjected to BPF, had a dramatic increase in  $b_H$  of  $0.4 \text{ d}^{-1}$ , doubling that of the control and acute test at  $0.2 \text{ d}^{-1}$ . The activity of the biomass was only slightly reduced from BPF at 53% compared to 54% of the acute and control (*Table 9*). When studying the model simulation of the COD profiles of acute and chronic BPF, it can be seen that the consumption rate of both  $S_S$  and  $S_H$  were reduced (*Figure 29*).

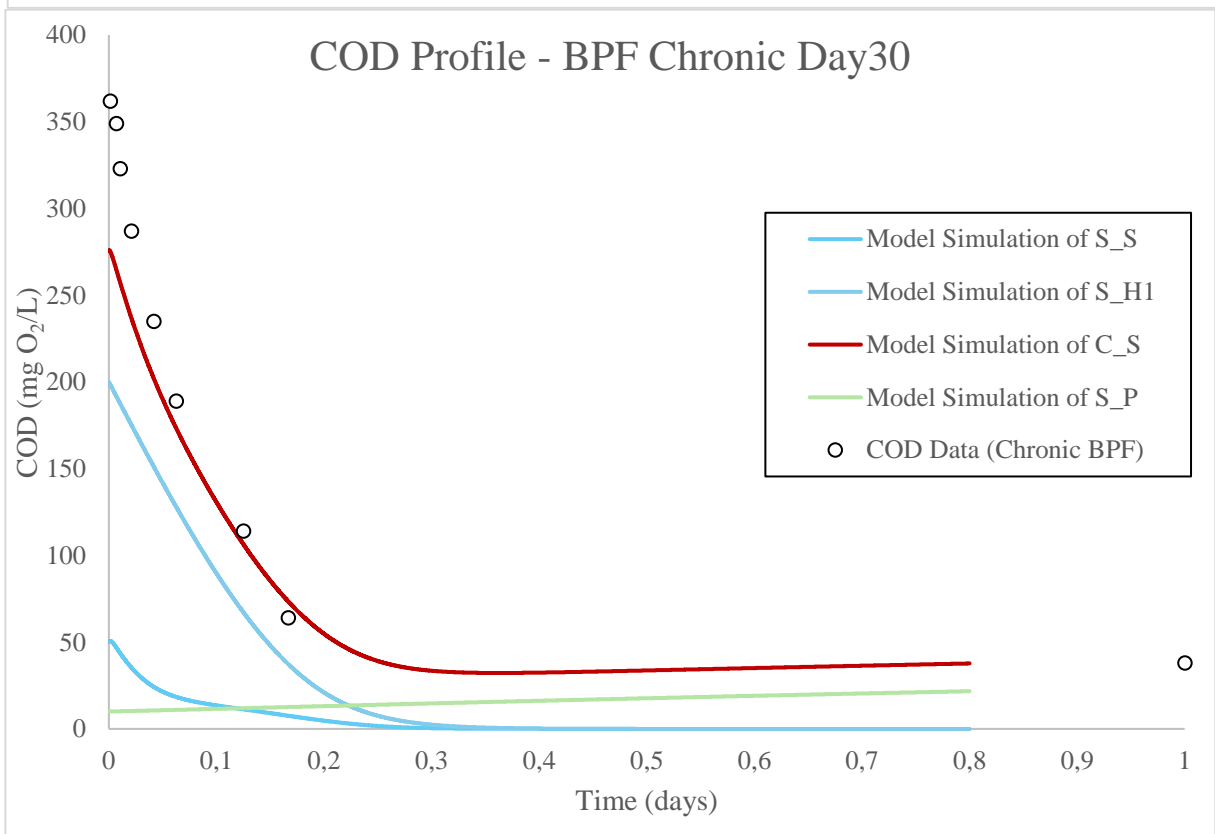
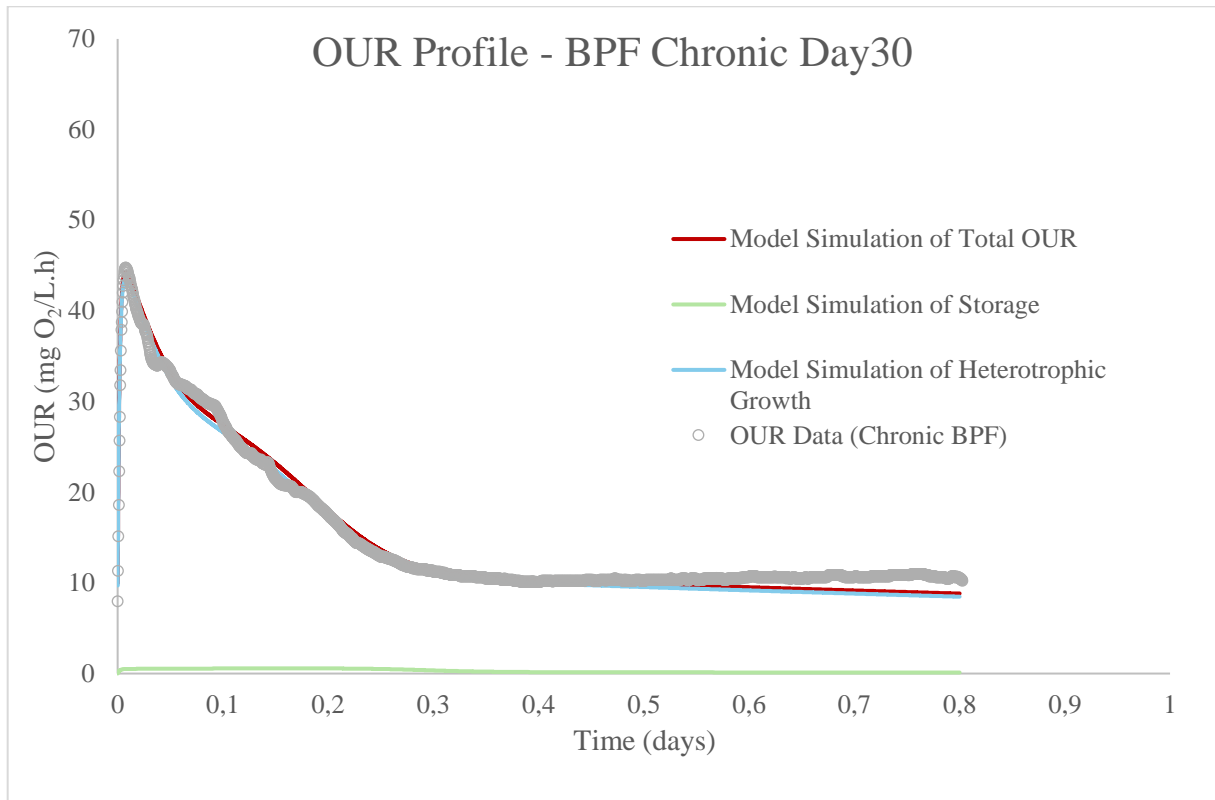


Figure 29 - Model simulation for OUR (Top) and COD (Bottom) Profiles of Chr. BPF test

The model calibration for chronic BPS inhibition shows that  $\hat{\mu}_H$  was dramatically affected during the chronic period, decreasing to  $1.1 \text{ d}^{-1}$  from  $3.5 \text{ d}^{-1}$  of the acute BPS test. As for chronic BPA,  $K_S$  had also decreased to  $1 \text{ mg COD/L}$  compared to  $35$  and  $25 \text{ mg COD/L}$  for the acute BPS and control test. Hydrolysis kinetics changed only slightly during the chronic period, having both  $k_H$  and  $K_X$  increase compared with the acute test. Nevertheless, the parameters were approximately half of the control and hydrolysis was still inhibited un-competitively. When examining storage on PHA's, it was found that  $k_{STO}$  only slightly increase while  $\hat{\mu}_{STO}$  was significantly reduced compared with acute BPS addition. Consequently, BPS had a non-competitive impact on the inhibition of PHA storage as  $K_{STO}$  was still yet unaffected and  $k_{STO}$  was still under half of the control. The decay rate,  $b_H$ , had increased during chronic subjection of BPS to  $0.31$  compared with  $0.2$  of the acute and control tests. The activity of the biomass had decreased slightly to  $52\%$  of the recorded  $54\%$  in the previously mentioned tests (*Table 9*). Examining the model simulation of the COD profiles of acute and chronic BPS, it can be seen that the consumption rate of  $S_S$  had increased slightly while the rate of consumption of  $S_H$  decreased (*Figure 30*).

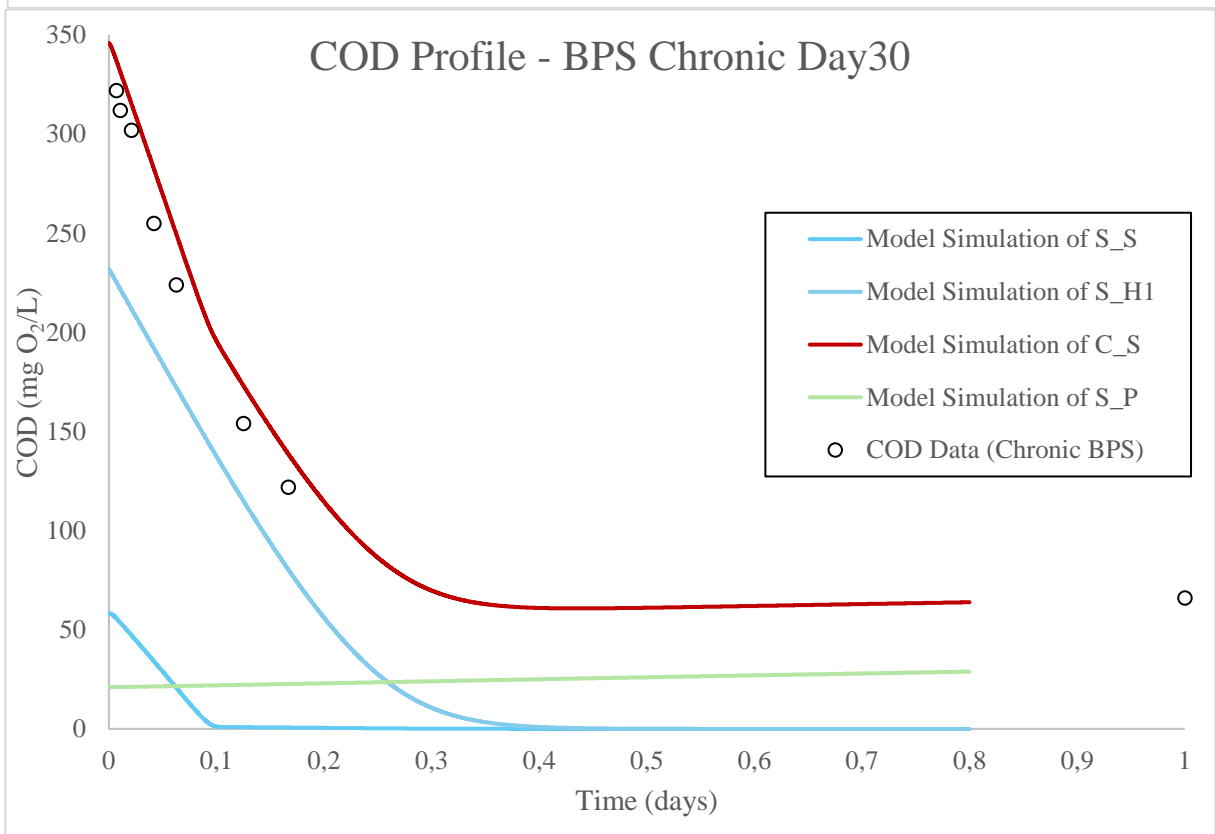
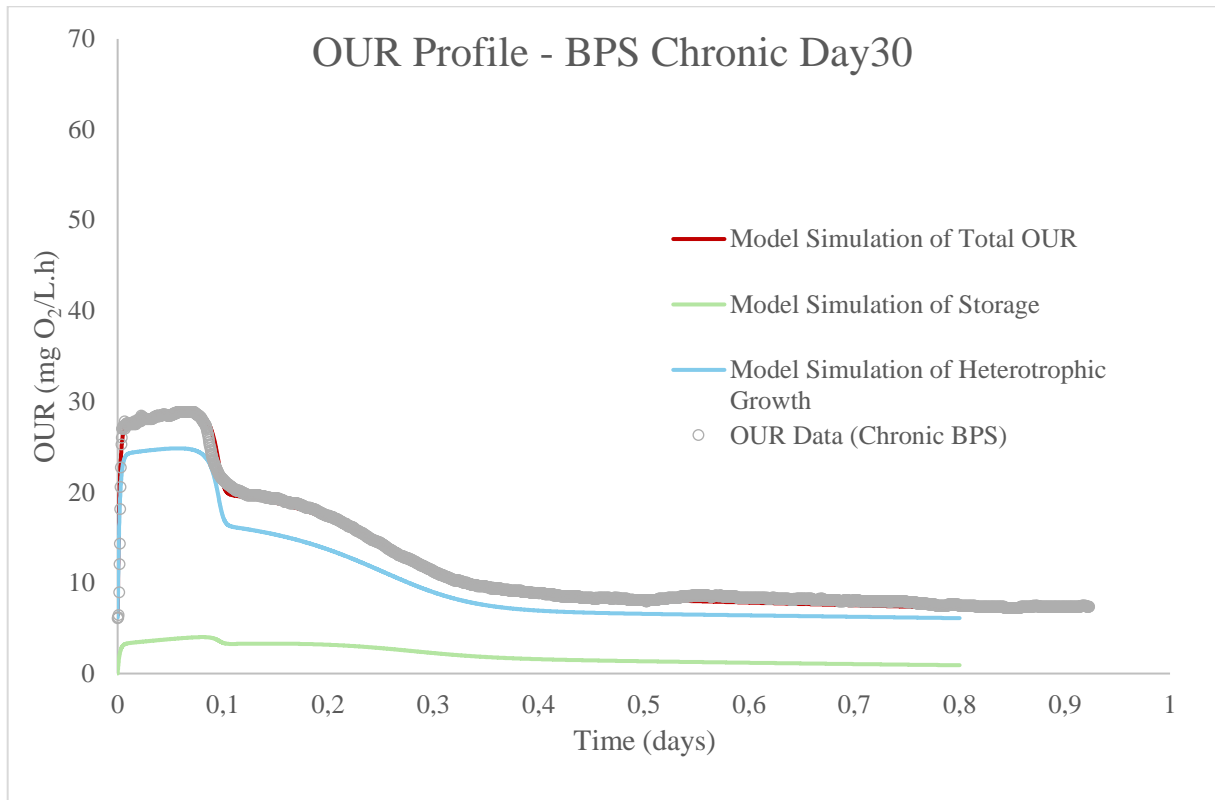


Figure 30 - Model simulation for OUR (Top) and COD (Bottom) Profiles of Chr. BPS test



Table 9 - Values of chronic models determined by model calibration

Model Parameters	Unit	Control	Chronic-BPS	Chronic-BPF	Chronic-BPA
Maximum growth rate for $X_H$	$\hat{\mu}_H$ 1/day	3.5	<b>1.1</b>	3.5	<b>1.15</b>
Half saturation constant for growth of $X_H$	$K_S$ mg COD/L	25	<b>1</b>	<b>50</b>	<b>1</b>
Maximum hydrolysis rate for $S_H$	$k_h$ 1/day	4.2	<b>1.83</b>	<b>2.17</b>	<b>2.26</b>
Hydrolysis half saturation constant for $S_H$	$K_X$ g COD/g COD	0.14	<b>0.058</b>	<b>0.089</b>	<b>0.09</b>
Maximum storage rate of PHA by $X_H$	$k_{STO}$	2	<b>0.8</b>	<b>0.1</b>	<b>1</b>
Half saturation constant for storage of PHA by $X_H$	$K_{STO}$	0.5	0.5	0.5	0.5
Maximum growth rate for $X_H$ on PHA	$\hat{\mu}_{STO}$	1.85	<b>0.5</b>	<b>0.1</b>	<b>1</b>
Endogenous decay rate for $X_H$	$b_H$ 1/day	0.2	<b>0.31</b>	<b>0.4</b>	<b>0.4</b>
Yield coefficient for $X_H$	$Y_H$ g COD/g COD	0.60	0.60	0.60	0.60
Yield coefficient for storage of PHA	$Y_{STO}$	0.85	0.85	0.85	0.85
Total biomass	mg VSS/L	1164	810	975	750
	mg COD/L	1653	1150	1384	1065
Initial active biomass	$X_H$ mg COD/L	885	600	730	500
Activity	%	54	52	53	<b>47</b>
Initial amount of biodegradable COD	$C_{SI}$ mg COD/L	250	290	250	315
Initial amount of readily biodegradable COD	$S_{SI}$ mg COD/L	50 (20%)	58	50	63
Initial amount of readily hydrolysable COD	$S_H$ mg COD/L	200 (80%)	232	200	252

## 5. Conclusions and Future Recommendations

The objective of this thesis was to determine the acute and chronic impact of BP analogues on the biomass in a wastewater treatment system using respirometry. The results found shows that all the BP analogues tested, both acute and chronic, have negative effects of growth, hydrolysis and storage of microorganisms found in a WWTP. Furthermore, when the OUR profiles are simulated using Aquasim based on ASM3, it was found that all BP analogues tested showed competitive inhibition for growth, un-competitive inhibition for hydrolysis and non-competitive inhibition for storage of PHA's. During chronic exposure of BPA and BPS, caused un-competitive inhibition for growth and hydrolysis and competitive inhibition for BPF. All BP analogues tested showed non-competitive inhibition for storage of PHA's. Additional effects are an increase in endogenous decay rate and loss of activity of the biomass. Looking at the concentration of solids and COD removal, it can be seen that chronic addition of all the BP analogues tested decreased the solids concentration and efficiency of COD removal. During the chronic period, degradation of the tested BP analogues was not observed. Acute and chronic exposure of BPF and BPS seemed to have an equal or worse effect on the organisms than the use of BPA.

Future recommendations of research include testing the microorganisms on BP analogues with lower SRT such as 2 days. Additionally, using field relevant concentrations of the tested BP analogues should be performed to accurately determine the impact of the BP analogues in a WWTP. This research should be considered significant as the reduced use of BPA incentivizes producers to use other, related plastic monomers.

## 6. References

- (1) Sepe, M. *Tracing the History of Polymeric Materials: Polycarbonate*. *Plastics Technology*, 2021. <https://www.ptonline.com/articles/tracing-the-history-of-polymeric-materials-part-11> (accessed 2021 18.4).
- (2) Vandenberg, L. N.; Hauser, R.; Marcus, M.; Olea, N.; Welshons, W. V. Human exposure to bisphenol A (BPA). *Reprod Toxicol* **2007**, *24* (2), 139-177. DOI: 10.1016/j.reprotox.2007.07.010 From NLM.
- (3) Centre, J. R.; Health, I. f.; Protection, C.; Olsson, H.; Aschberger, K.; Munn, S. *Updated European Union risk assessment report – 4,4'-isopropylidenediphenol (bisphenol-A) – Environment addendum of February 2008*; Publications Office, 2010. DOI: doi/10.2788/40195.
- (4) Bailin, P. D. B., M. & Lewis, S. & Liroff, Richard. Public awareness drives market for safer alternatives: bisphenol A market analysis report. *IEHN* **2008**, 37.
- (5) Rochester, J. R. Bisphenol A and human health: A review of the literature. *Reproductive Toxicology* **2013**, *42*, 132-155. DOI: <https://doi.org/10.1016/j.reprotox.2013.08.008>.
- (6) Moore, A. L. *Poisoned by Plastic: The Analysis of BPA and its Derivatives in Water Bottles*. 2016. <https://www.hamiltoncompany.com/laboratory-products/case-studies/poisoned-by-plastic-the-analysis-of-bpa-and-its-derivatives-in-water-bottles> (accessed 2024 18.4).
- (7) Jeon, G. W. Bisphenol A leaching from polycarbonate baby bottles into baby food causes potential health issues. *Clin Exp Pediatr* **2022**, *65* (9), 450-452. DOI: 10.3345/cep.2022.00661 From NLM.
- (8) Preksha Palsania, K. S., Mohd Ashaf Dar, Garima Kaushik. Food grade plastics and Bisphenol A: Associated risks, toxicity, and bioremediation approaches. *Journal of Hazardous Materials* **2024**, 466. DOI: <https://doi.org/10.1016/j.jhazmat.2024.133474>.
- (9) Lambré, C.; Barat Baviera, J. M.; Bolognesi, C.; Chesson, A.; Cocconcelli, P. S.; Crebelli, R.; Gott, D. M.; Grob, K.; Lampi, E.; Mengelers, M.; et al. Re-evaluation of the risks to public health related to the presence of bisphenol A (BPA) in foodstuffs. *Efsa j* **2023**, *21* (4), e06857. DOI: 10.2903/j.efsa.2023.6857 From NLM.
- (10) Liao, C.; Liu, F.; Kannan, K. Bisphenol S, a New Bisphenol Analogue, in Paper Products and Currency Bills and Its Association with Bisphenol A Residues. *Environmental Science & Technology* **2012**, *46* (12), 6515-6522. DOI: 10.1021/es300876n.
- (11) Viñas, P.; Campillo, N.; Martínez-Castillo, N.; Hernández-Córdoba, M. Comparison of two derivatization-based methods for solid-phase microextraction–gas chromatography–mass spectrometric determination of bisphenol A, bisphenol S and biphenol migrated from food cans. *Analytical and Bioanalytical Chemistry* **2010**, *397* (1), 115-125. DOI: 10.1007/s00216-010-3464-7.
- (12) Lee, S.; Liao, C.; Song, G.-J.; Ra, K.; Kannan, K.; Moon, H.-B. Emission of bisphenol analogues including bisphenol A and bisphenol F from wastewater treatment plants in Korea. *Chemosphere* **2015**, *119*, 1000-1006. DOI: <https://doi.org/10.1016/j.chemosphere.2014.09.011>.
- (13) Yamazaki, E.; Yamashita, N.; Taniyasu, S.; Lam, J.; Lam, P. K. S.; Moon, H.-B.; Jeong, Y.; Kannan, P.; Achyuthan, H.; Munuswamy, N.; et al. Bisphenol A and other bisphenol analogues including BPS

and BPF in surface water samples from Japan, China, Korea and India. *Ecotoxicology and Environmental Safety* **2015**, 122, 565-572. DOI: <https://doi.org/10.1016/j.ecoenv.2015.09.029>.

(14) B, J. The water resources in Chennai: Cooum River. **2018**, 2, 21.

(15) Cabaton, N.; Dumont, C.; Severin, I.; Perdu, E.; Zalko, D.; Cherkaoui-Malki, M.; Chagnon, M.-C. Genotoxic and endocrine activities of bis(hydroxyphenyl)methane (bisphenol F) and its derivatives in the HepG2 cell line. *Toxicology* **2009**, 255 (1), 15-24. DOI: <https://doi.org/10.1016/j.tox.2008.09.024>.

(16) Xiaoliu Zhou, J. P. K., Antonia M. Calafat, Xiaoyun Ye. Automated on-line column-switching high performance liquid chromatography isotope dilution tandem mass spectrometry method for the quantification of bisphenol A, bisphenol F, bisphenol S, and 11 other phenols in urine,. *Journal of Chromatography B* **2014**, 944, 4. DOI: <https://doi.org/10.1016/j.jchromb.2013.11.009>.

(17) Mohammad, N.; Marian, Y. L. W.; Fatemeh, G. Developmental exposure of zebrafish (*Danio rerio*) to bisphenol-S impairs subsequent reproduction potential and hormonal balance in adults. *Aquatic Toxicology* **2014**, 148, 195-203. DOI: <https://doi.org/10.1016/j.aquatox.2014.01.009>.

(18) Stroheker, T.; Chagnon, M. C.; Pinnert, M. F.; Berges, R.; Canivenc-Lavier, M. C. Estrogenic effects of food wrap packaging xenoestrogens and flavonoids in female Wistar rats: a comparative study. *Reprod Toxicol* **2003**, 17 (4), 421-432. DOI: 10.1016/s0890-6238(03)00044-3 From NLM.

(19) Yamasaki, K.; Noda, S.; Imatanaka, N.; Yakabe, Y. Comparative study of the uterotrophic potency of 14 chemicals in a uterotrophic assay and their receptor-binding affinity. *Toxicol Lett* **2004**, 146 (2), 111-120. DOI: 10.1016/j.toxlet.2003.07.003 From NLM.

(20) Yamasaki, K.; Takeyoshi, M.; Sawaki, M.; Imatanaka, N.; Shinoda, K.; Takatsuki, M. Immature rat uterotrophic assay of 18 chemicals and Hershberger assay of 30 chemicals. *Toxicology* **2003**, 183 (1-3), 93-115. DOI: 10.1016/s0300-483x(02)00445-6 From NLM.

(21) Higashihara, N.; Shiraishi, K.; Miyata, K.; Oshima, Y.; Minobe, Y.; Yamasaki, K. Subacute oral toxicity study of bisphenol F based on the draft protocol for the "Enhanced OECD Test Guideline no. 407". *Arch Toxicol* **2007**, 81 (12), 825-832. DOI: 10.1007/s00204-007-0223-4 From NLM.

(22) Rochester, J. R.; Bolden, A. L. Bisphenol S and F: A Systematic Review and Comparison of the Hormonal Activity of Bisphenol A Substitutes. *Environ Health Perspect* **2015**, 123 (7), 643-650. DOI: 10.1289/ehp.1408989 From NLM.

(23) Wolfgang Dekant, W. V. Human exposure to bisphenol A by biomonitoring: Methods, results and assessment of environmental exposures,. *Toxicology and Applied Pharmacology* **2008**, 228 (1), 20. DOI: <https://doi.org/10.1016/j.taap.2007.12.008>.

(24) Kurebayashi, H., Nagatsuka, Shin-Ichiro, Nemoto, Hiroyuki, Noguchi, Hideyo, Ohno, Yasuo. Disposition of low doses of <sup>14</sup>C-bisphenol A in male, female, pregnant, fetal, and neonatal rats. *Archives of Toxicology* **2005**, 79 (5), 10. DOI: 10.1007/s00204-004-0628-2.

(25) Cabaton, N.; Chagnon, M. C.; Lhuguenot, J. C.; Cravedi, J. P.; Zalko, D. Disposition and metabolic profiling of bisphenol F in pregnant and nonpregnant rats. *J Agric Food Chem* **2006**, 54 (26), 10307-10314. DOI: 10.1021/jf062250q From NLM.

(26) Ike, M.; Jin, C. S.; Fujita, M. Biodegradation of bisphenol A in the aquatic environment ., *Water science and technology* **2000**, 42 (7-8), 31--38.

- (27) Spivack, J.; Leib, T.; Lobos, J. Novel pathway for bacterial metabolism of bisphenol A. Rearrangements and stilbene cleavage in bisphenol A metabolism. *Journal of Biological Chemistry* **1994**, *269* (10), 7323-7329.
- (28) Eltoukhy, A., Jia, Y., Nahurira, R. et al. Eltoukhy, A., Jia, Y., Nahurira, R. et al. *BMC Microbiology* **2020**, *20* (1). DOI: 10.1186/s12866-020-1699-9.
- (29) Ana, K.; Celine, G.; Martin Rafael, G.; Tjaša, G.; Tina, K.; David, H.; Adrian, C.; Ester, H. Kinetics and biotransformation products of bisphenol F and S during aerobic degradation with activated sludge. *Journal of Hazardous Materials* **2021**, *404*. DOI: <https://doi.org/10.1016/j.jhazmat.2020.124079>.
- (30) Metcalf & Eddy, I. *Wastewater Engineering: Treatment and Resource Recovery*; 2014.
- (31) Henze, M. Modeling of Aerobic Wastewater Treatment Processes. In *Environmental Biotechnology: Concepts and Applications*, Winter, H.-J. J. a. J. Ed.; WILEY-VCH Verlag, 2005; p 14.
- (32) Ozkok, I. P. INHIBITORY IMPACT OF SELECTED ANTIBIOTICS ON BIODEGRADATION CHARACTERISTIC AND MICROBIAL POPULATION UNDER AEROBIC CONDITIONS. Istanbul Technical University, 2012.
- (33) Orhon, D.; Artan, N. *Modelling of activated sludge systems*; Technomic Publ. Co., 1994.
- (34) Gujer, W., Henze, M., Mino, T. and Loosdrecht M.v. Activated Sludge Model No. 3. *Water Sci. Tech.* **1999**, *39*, 11.
- (35) Dircks, K.; Beun, J. J.; van Loosdrecht, M.; Heijnen, J. J.; Henze, M. Glycogen metabolism in aerobic mixed cultures. *Biotechnol Bioeng* **2001**, *73* (2), 85-94. DOI: 10.1002/bit.1040 From NLM.
- (36) Reis, M. A.; Serafim, L. S.; Lemos, P. C.; Ramos, A. M.; Aguiar, F. R.; Van Loosdrecht, M. C. Production of polyhydroxyalkanoates by mixed microbial cultures. *Bioprocess Biosyst Eng* **2003**, *25* (6), 377-385. DOI: 10.1007/s00449-003-0322-4 From NLM.
- (37) M<sup>a</sup>D. Coello Oviedo, J. B. S. C. A. C.; Alonso, J. M. Q. A new approach to toxicity determination by respirometry. *Environmental Technology* **2009**, *30* (14), 1601--1605. DOI: 10.1080/09593330903358294 , note = PMID: 20184005.
- (38) Agnieszka, C.-K.; Magdalena, Z.; Katarzyna, B.; Katarzyna, B.; Irena, W.-B. Insights into mechanisms of bisphenol A biodegradation in aerobic granular sludge. *Bioresource Technology* **2020**, *315*, 123806. DOI: <https://doi.org/10.1016/j.biortech.2020.123806>.
- (39) Oliveira Pereira, E. A.; Labine, L. M.; Kleywegt, S.; Jobst, K. J.; Simpson, A. J.; Simpson, M. J. Metabolomics Reveals That Bisphenol Pollutants Impair Protein Synthesis-Related Pathways in *Daphnia magna*. *Metabolites* **2021**, *11* (10). DOI: 10.3390/metabo11100666 From NLM.
- (40) Anak Juan, D.; Abu Hasan, H.; Muhamad, M. H.; Sheikh Abdullah, S. R.; Abu Bakar, S. N. H.; Buhari, J. Physico-Chemical and Biological Techniques of Bisphenol a Removal in Aqueous Solution.

*Journal of Ecological Engineering* **2021**, 22 (9), 136-148, journal article. DOI: 10.12911/22998993/141333.

(41) ISO. *ISO 8192:2007*; 2007.

(42) Scientific, F. *Standard Operating Procedure for: Total Suspended Solids*; 2007.

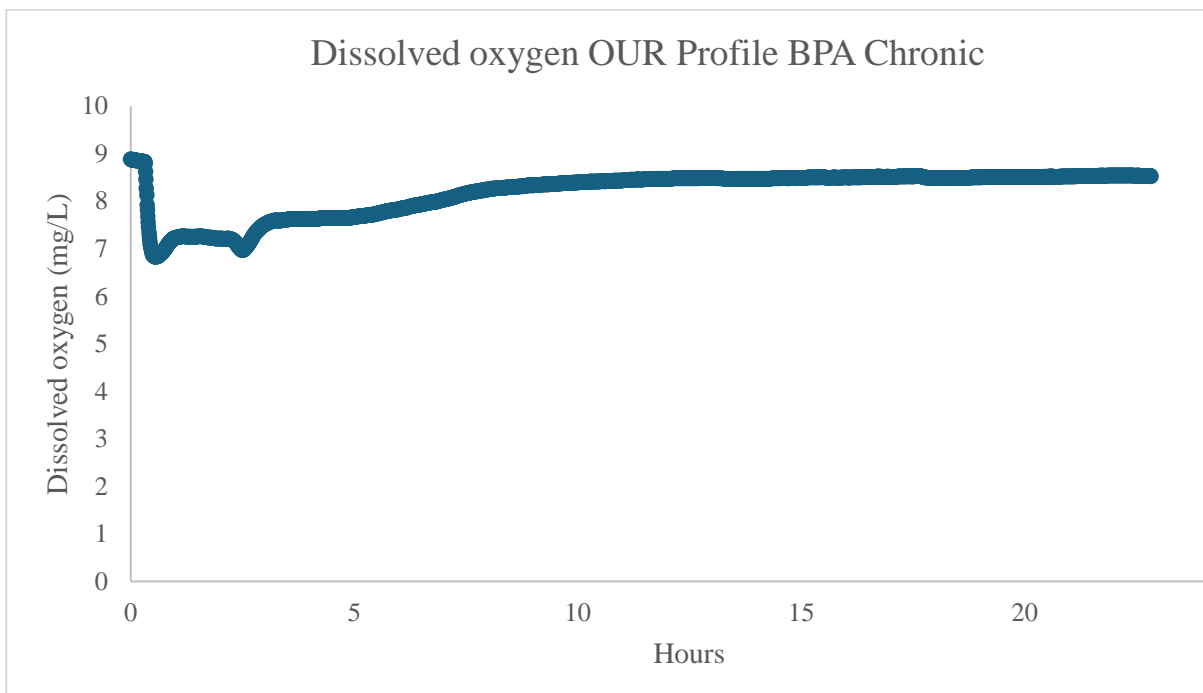
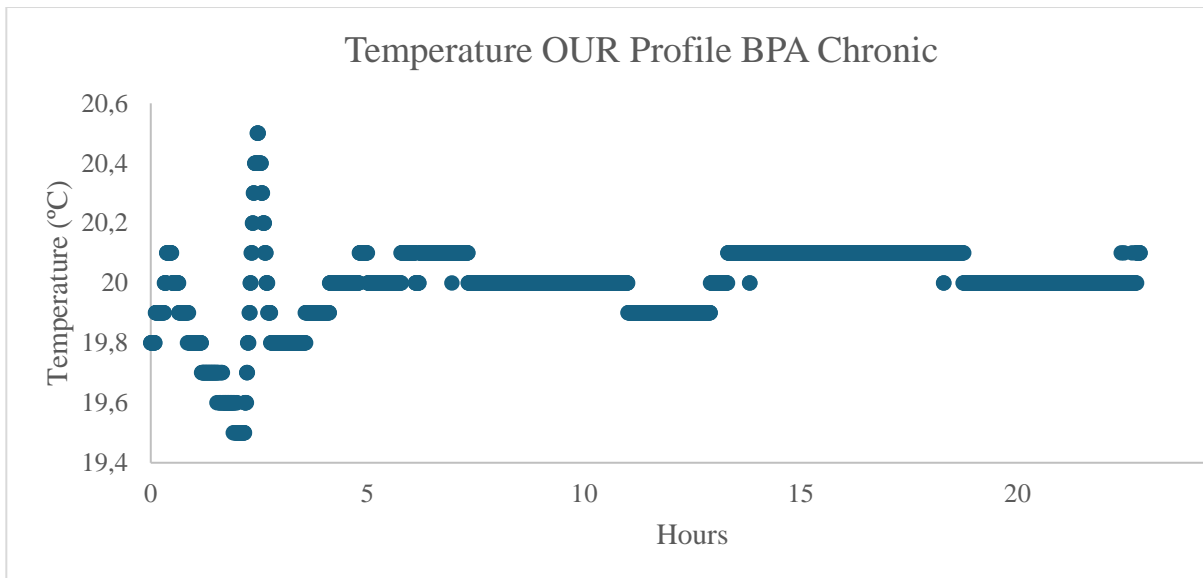
(43) EPA, U. pH ELECTROMETRIC MEASUREMENT. **2004**, 5.

(44) Grendal, M. G. Acute impact of Bisphenol-A Alternatives on the Activated Sludge Biomass. Bachelor, University of Stavanger, Stavanger, 2019.

(45) Ferrer-Polonio, E.; Alvim, C. B.; Fernández-Navarro, J.; Mompó-Curell, R.; Mendoza-Roca, J. A.; Bes-Piá, A.; Alonso-Molina, J. L.; Amorós-Muñoz, I. Influence of bisphenol A occurrence in wastewaters on biomass characteristics and activated sludge process performance. *Science of The Total Environment* **2021**, 778, 146355. DOI: <https://doi.org/10.1016/j.scitotenv.2021.146355>.

## 7. Appendix

The temperature, dissolved oxygen and OUR profile gained from the chronic OUR experiments are given in Figure 31, Figure 32 and Figure 33 for BPA, BPF and BPS, respectively.



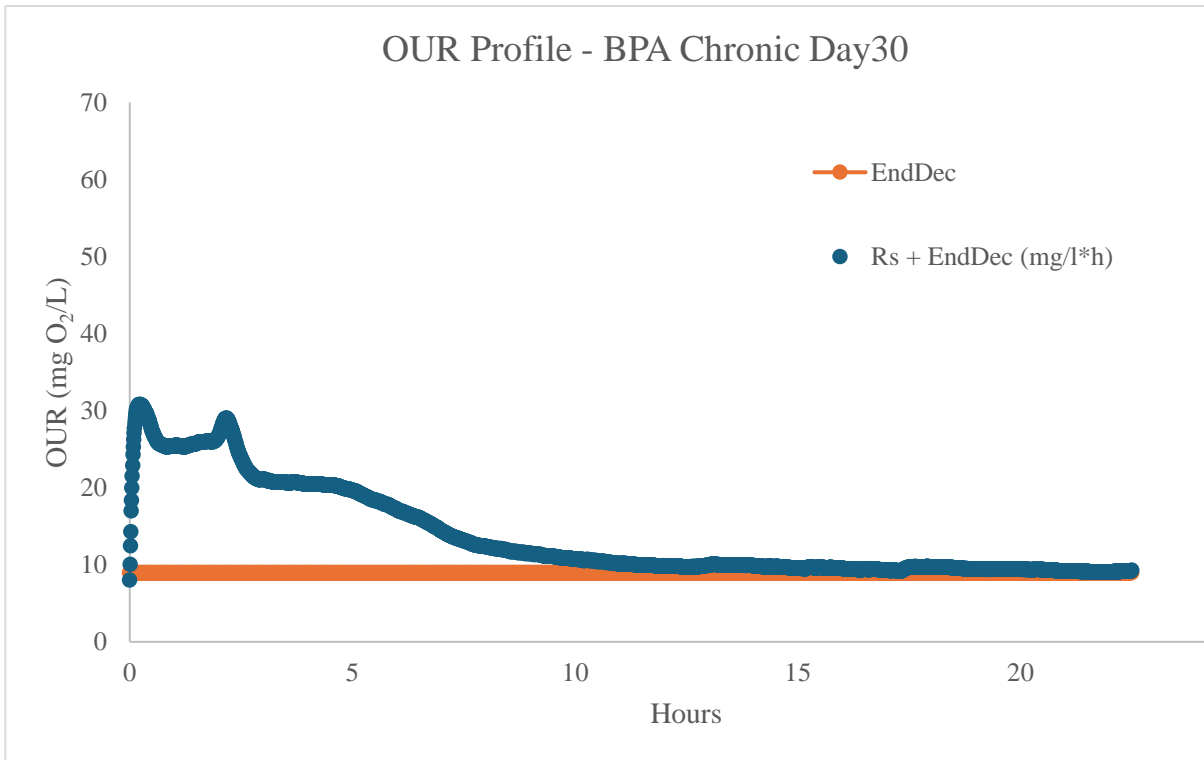
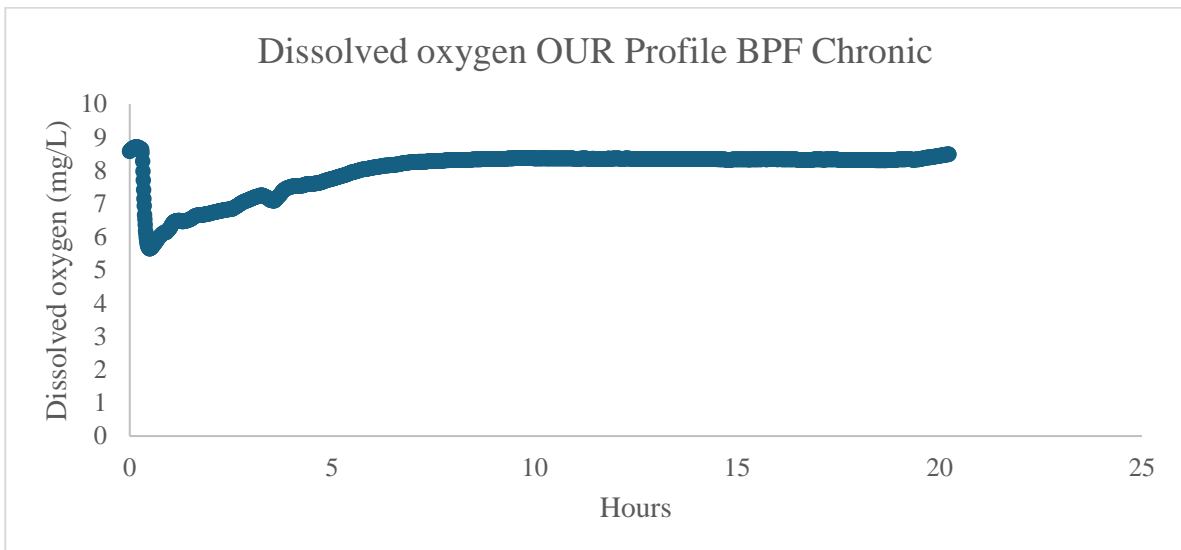
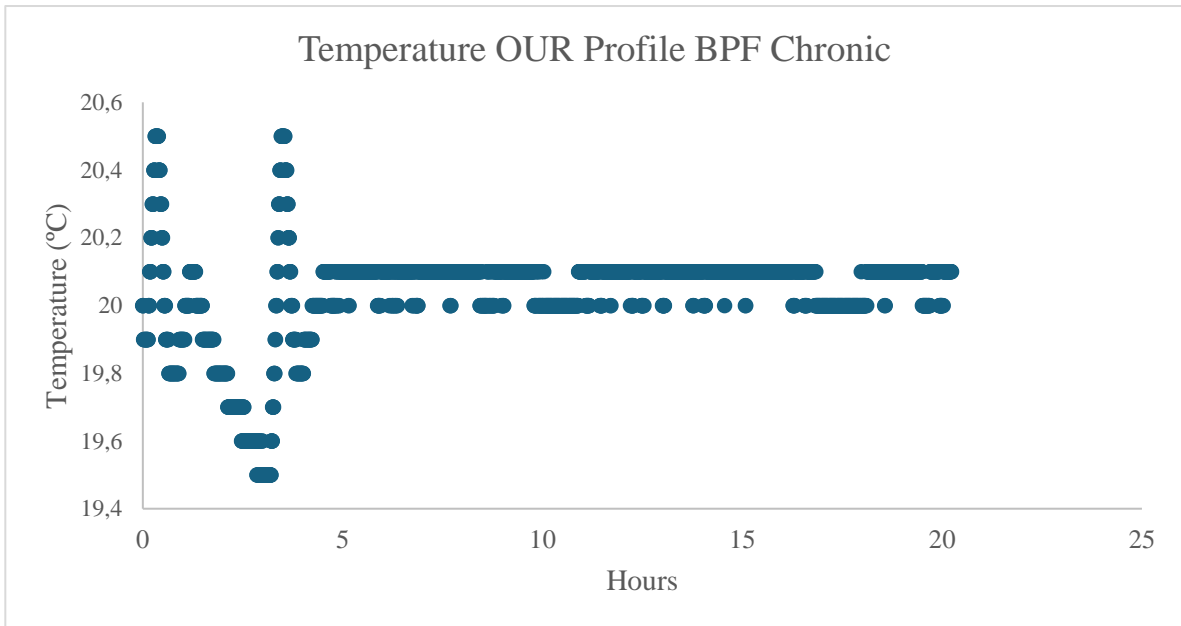


Figure 31 – Temp. (Top), DO (Middle) and OUR (Bottom) Profiles from Chr. BPA test





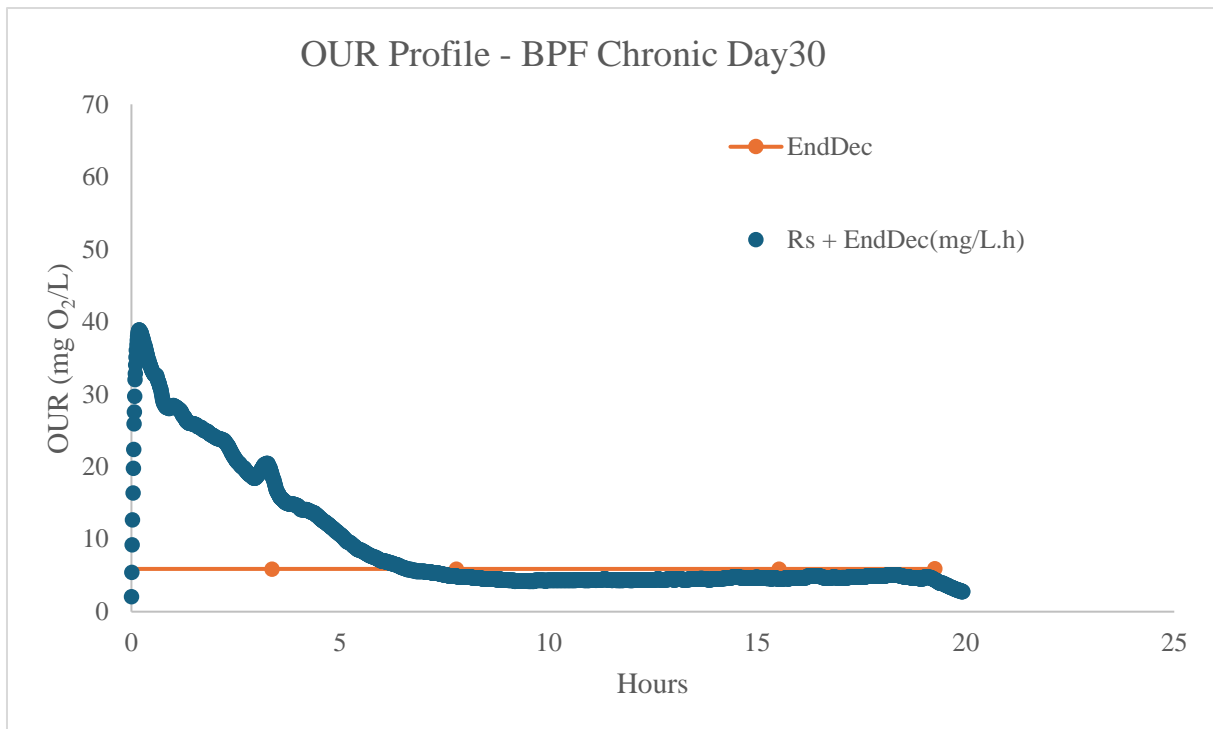
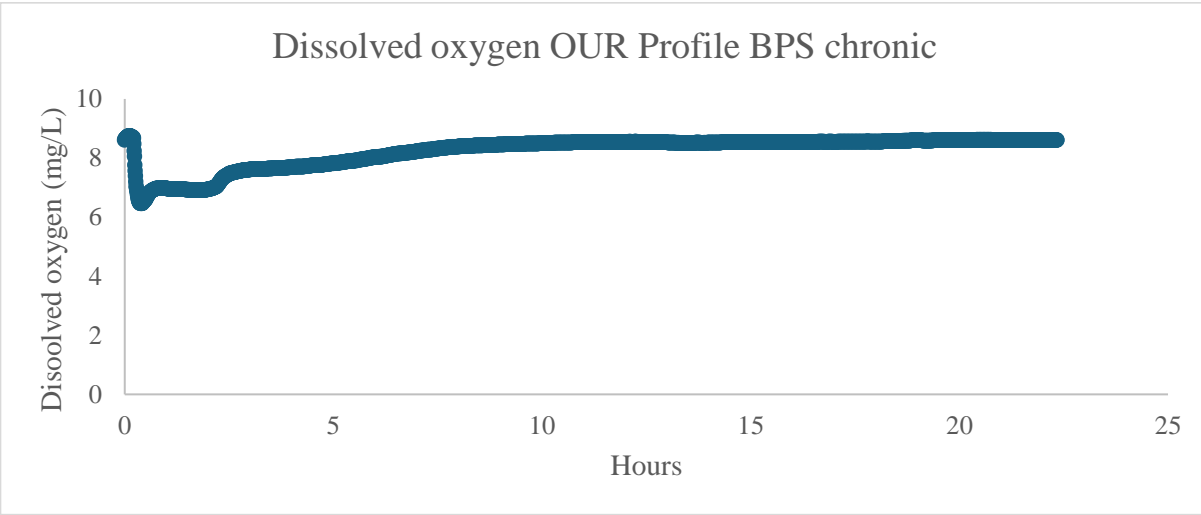
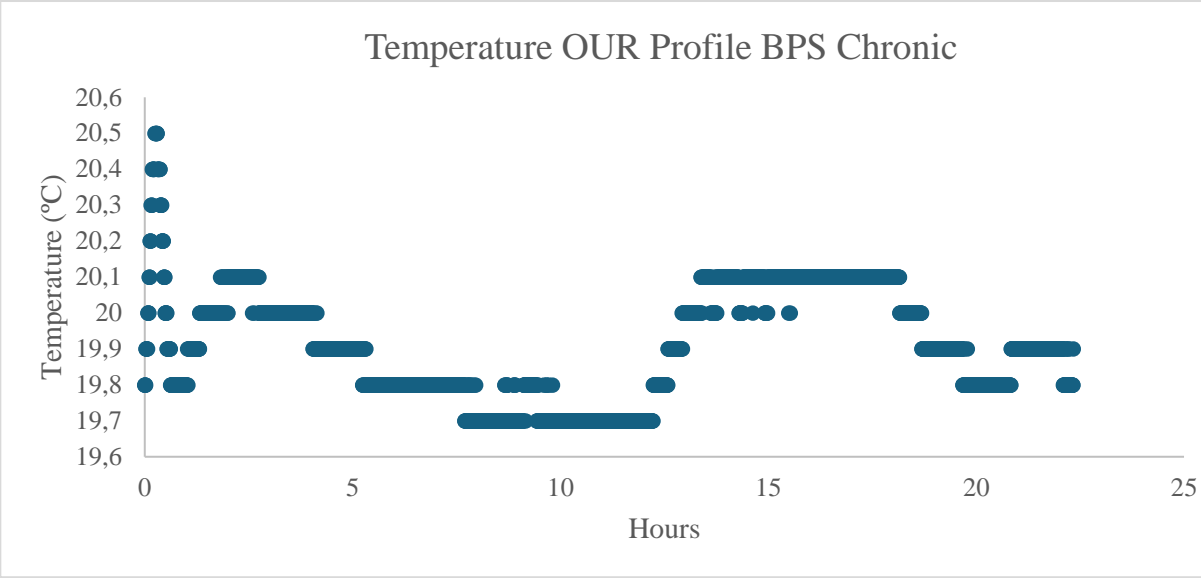


Figure 32 – Temp. (Top), DO (Middle) and OUR (Bottom) Profiles from Chr. BPF test



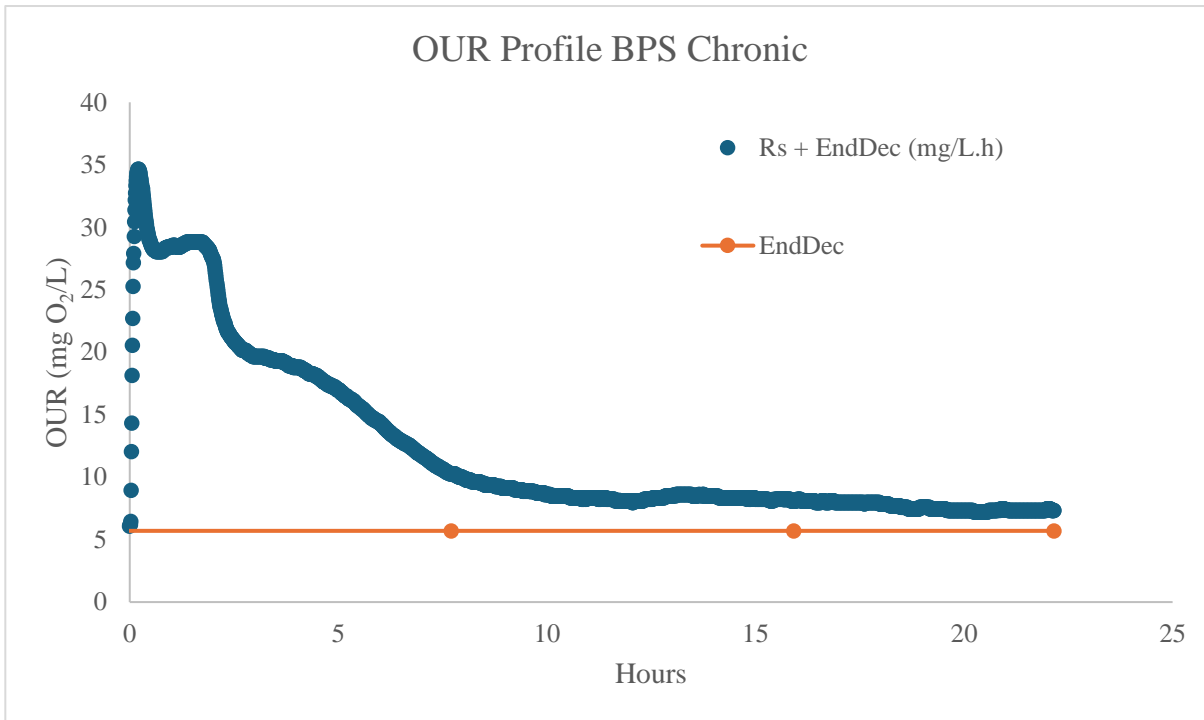


Figure 33 – Temp. (Top), DO (Middle) and OUR (Bottom) Profiles from Chr. BPS test